Philips Technical Review

MEASURING METHODS FOR SOME PROPERTIES OF FERROXCUBE MATERIALS

by C. M. van der BURGT, M. GEVERS and H. P. J. WIJN.   621.318.134: 621.317.4

Ferroxcube materials differ from other soft ferromagnetic materials in that they are especially suitable for use at high frequencies. For this reason, in the measurement of their characteristics, methods are applied which for the greater part belong to those commonly used in radio- and radar-technique, and are thus rather unusual in the field of ferromagnetism.

Introduction

The technically most important properties of a soft ferromagnetic material are the permeability and the losses in an alternating field. These quantities, for Ferroxcube materials, have been amply dealt with in an earlier article in this Review [1]. In this article, the discussion of the two quantities was divided into two sections, which dealt with the behaviour in weak and in strong fields respectively. The reason for this separation was principally that the magnetization process, for sufficiently weak fields, may be considered to be fairly closely reversible. In other words, the hysteresis phenomenon has in this case no noticeable influence and makes therefore only a negligibly small contribution to the losses. The behaviour in weak fields is thus easily understood, and the entire behaviour below the frequency range in which ferromagnetic resonance occurs, insofar as permeability and losses are concerned, is described by a complex material constant, the complex initial permeability

$$\mu_i = \mu_i' - j\mu_i'' \quad \cdots \cdots \quad (1)$$

(in fact there are thus two real quantities μ_i' and μ_i'' requisite for a full description). As was amply described in I, the behaviour in strong fields is considerably more complicated, since the real part of the permeability and the losses at all fre-

quencies depend both on the frequency and on the field strength. In that case the properties mentioned must be derived from the magnetization curves (I, figs 7 and 8), the curves for the total losses (I, fig. 9) and the curves for the distortion.

The determination of the permeability and losses of metallic ferromagnetic materials is more complicated, as compared with Ferroxcube, by the fact that, as a consequence of their low resistivity, a high-frequency magnetic field has only a small depth of penetration (skin-effect): as a result, a certain effective permeability is measured, which is dependent on the shape and dimensions of the piece of metal. If it is desired to derive from this "effective" permeability the "true" permeability, which is a true material property independent of the shape, the skin-effect must be introduced quantitatively into the calculations, which naturally involves a certain amount of complication.

The occurrence of the skin effect in metals has the consequence that the losses are chiefly due to eddy currents. The completely different situation with regard to losses which is found when dealing with Ferroxcube has already been amply discussed in I, as also in a later article dealing with the applications of Ferroxcube materials [2].

In the present article we will give a review of the methods available for the measurement of various

---

[1] J. J. Went and E. W. Gorter, Philips tech. Rev. 13, 181, 1952 (No. 7), referred to in the following as I. The system of rationalized Giorgi units will be used also in the present article. The permeability of the vacuum is then $\mu_0 = 4\pi \cdot 10^{-7}$ H/m.

[2] W. Six, Philips tech. Rev. 13, 301, 1952 (No. 11), referred to in the following as II.

properties of Ferroxcube materials, such as those mentioned above, when subjected to a purely sinusoidal, alternating field. As in I, a distinction will be made between measurements in weak fields and measurements in strong fields. For both cases further consideration will be given to the methods of measuring the permeability and losses. Finally, we shall also discuss the measurement of the magnetization curve and the distortion, the importance of which was clearly shown in II.

In all these considerations we shall refrain from going into details of the measuring equipment, but limit ourselves to the examination of the relative merits of the different methods available. It will frequently be necessary to employ different methods for the determination of the same quantity, according to the frequency and the field strength at which the measurements are to be made, and the order of magnitude of the quantity to be measured in the given circumstances.

Recapitulation of certain concepts

Permeability and losses in weak fields

To obtain a better insight, we shall note here the most important definitions bearing on the concepts of permeability and losses. For a fuller discussion the reader is referred to I and II.

If Ferroxcube is employed as core material in an ideal toroid, and if a weak uniform magnetic field H is excited by means of a weak current, passing through the toroid and varying purely sinusoidally with time, then the flux density B is nearly enough a linear function of the field H. As a consequence of the losses occurring in the ferromagnetic material (in this case, to a close approximation, exclusively "residual losses"), a phase difference appears between B and H. The relation between B and H is given by $B = \mu_i H$, in which μ_i is the previously mentioned, complex, initial permeability (formula 1). The phase angle δ_F between B and H is now given by

$$\tan \delta_F = \frac{\mu_i''}{\mu_i'} \quad \ldots \ldots \ldots \quad (2)$$

As was amply described in II, this method of description amounts to replacing the coil and core by a loss-free coil with inductance L_s and a resistance R_s connected in series. For an ideal toroid of length l (measured along the centre line), cross-section O and number of turns n, which closely surrounds a core of ferromagnetic material with (complex) initial permeability μ_i, the following equations apply:

$$R_s = \omega n^2 \frac{O}{l} \mu_i'', \quad \ldots \ldots \quad (3)$$

$$L_s = n^2 \frac{O}{l} \mu_i'. \quad \ldots \ldots \quad (4)$$

In these equations ω is the angular velocity of the sinusoidally alternating field.

Permeability and losses in strong fields

At high values of the flux density, the permeability and losses cannot be described by a complex permeability $\mu = \mu' - j\mu''$. In the first place, at high values, the relationship $B = \mu H$ is no longer fully valid, even if μ is assumed to be dependent on the frequency and the peak value of the flux density. This is associated with the distortion (to be discussed more fully later) whereby a field H which varies purely sinusoidally with time, produces a non-sinusoidal flux density B. In the second place, the use of a permeability μ would not result in any simplification, since this quantity would depend too closely on the frequency and the flux density. The behaviour of Ferroxcube can thus not be described in a simple manner in the case of strong fields, as is possible with weak fields. As already mentioned in the introduction, recourse must be had to graphical representations: one giving the relationship between the amplitudes B_m and H_m for various frequencies, another from which can be read the power dissipated by a sinusoidally alternating field in a Ferroxcube core, per unit volume, as a function of the maximum flux density in the core (see I, figs 7, 8 and 9), and finally a further figure giving the distortion as a function of frequency and maximum field strength.
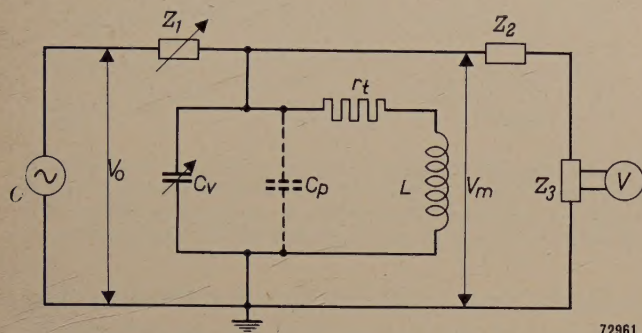
Measurement of permeability and losses in "weak" fields

Measurements at low frequencies (50 kc/s—10 Mc/s)

The most obvious manner of determining the quantities μ_i' and μ_i'' at relatively low frequencies (e.g. up to 10 Mc/s) follows directly from the definitions of these quantities and their relationship to the quantities R_s and L_s for a coil with a Ferroxcube core as given in the introduction. A number of turns of stranded copper wire are wound on a previously demagnetized ring of square or circular cross-section, made of the material to be investigated. The inductance L_s and the series resistance R_s of the resulting coil are measured by means of a bridge circuit, from which, by use of formulae (3) and (4) — the dimensions of the ring and the number of turns being known — μ_i' and μ_i'' may

be calculated. In such a measurement it must be remembered that the stray capacitance C_p of the winding on the core interferes with the direct measurement of the values R_s and L_s. The values found are, $R_s/(1—\omega^2 L_s C_p)^2$ and $L_s/(1—\omega^2 L_s C_p)$, provided that both $\omega^2 L_s C_p$ and $\omega^2 L_s C_p \tan \delta_t$ are small compared with unity.

A method whereby the series inductance and the tangent of the loss angle may be measured directly is the following resonance method, which may be applied, in general, in the frequency range between 50 kc/s and 10 Mc/s (see *fig. 1*).

Fig. 1. Diagram of the resonance method for the determination of μ' and μ'' in "weak" fields and at "low" frequencies. O oscillator, C_v variable capacitance for the tuning of the resonant circuit, L inductance, r_t equivalent resistance for the total losses in the resonance circuit, C_p stray capacitance, V voltmeter.

An accurately calibrated oscillator (O) is coupled via a large impedance Z_1 to a tuned circuit. The output voltage V_0 of the oscillator is independent of the frequency and of the impedance of the measuring circuit. The voltage V_m across the tuned circuit is measured by an electronic voltmeter (V), which is very loosely coupled to the tuned circuit of impedance Z via the impedance Z_2 and its own input impedance Z_3. If $Z_1 \gg Z$ and also $Z_2 \gg Z$, then the current i through the measuring circuit is, in close approximation, determined exclusively by the magnitude of Z_1, and at the same time the voltage V_m across the tuned circuit is determined exclusively by i and the magnitude of Z.

The tuned circuit itself comprises the following elements: the toroid, with a Ferroxcube core and inductance L_s, and a resistance r_t representing all the losses in the tuned circuit, a variable capacitor with capacitance C_v serving for the tuning of the circuit, to which must be added the stray capacitance C_p of the coil with core.

The resistance r_t comprises the various components:

$$r_t = r_F + r_D + r_K, \quad \ldots \ldots \quad (5)$$

in which r_F represents the ferromagnetic losses

occurring in the core, r_D the dielectric losses in the core, and r_K the I^2R losses in the winding. If the losses are small, according to (5) the following relation also holds:

$$\tan \delta_t = r_t/\omega L_s = \tan \delta_F + \tan \delta_D + \tan \delta_K. \quad (6)$$

The measurements are now carried out as follows: the value $C_v{}^0$ of C_v is determined, for which, at a given oscillator frequency, the voltage across the tuned circuit is at a maximum. We thus obtain $C_v{}^0$ from the condition:

$$\frac{d|Z|^2}{dC_v} = 0,$$

in which:

$$Z = \frac{(r_t + j\omega L_s)/j\omega C_t}{r_t + j\omega L_s + 1/j\omega C_t} \quad \text{and} \quad C_t = C_v + C_p.$$

$C_v{}^0$ is then given by:

$$\omega^2 L_s C_t{}^0 = \frac{1}{1 + \tan^2 \delta_t},$$

where $C_t{}^0 = C_v{}^0 + C_p$ and $\tan \delta_t = r_t/\omega L_s$. If $\tan^2 \delta_t$ is neglected in comparison with unity, we derive the inductance desired from the resonance capacitance $C_v{}^0$ by:

$$L_s = \frac{1}{\omega^2 (C_v{}^0 + C_p)}. \quad \ldots \ldots \quad (7)$$

We then find the loss angle δ_t by determining the difference ΔC_v between the two values of C_v for which the impedance of the tuned circuit is exactly $1/\sqrt{2}$ times the maximum value. ΔC_v is also known as the resonance width. The following now holds:

$$\tan \delta_t = \Delta C_v/2(C_v{}^0 + C_p) \quad \ldots \quad (8)$$

The limitations of and sources of error in the method described are the following. In the first place $\tan \delta_t$ must always be **small**, as otherwise the resonance curve will be too flat, so that the resonance value $C_v{}^0$ of the measuring capacitor can no longer be determined with sufficient accuracy. In addition, the **stray capacitance** C_p of the winding, unless this capacitance is separately measured and allowed for in the calculations, introduces errors in the computed values of the inductance and $\tan \delta_t$; this is obvious from formula (7). From the same formula it can also be seen that the stray capacitance prevents any determination of L_s above a certain frequency, since (7) may be expressed as: $L_s \omega^2 C_t = L_s \omega^2 (C_v{}^0 + C_p) = 1$. Thus the value of the variable capacitance C_v at constant L_s decreases with increasing ω.

If the frequency is so high that $L_s \omega^2 C_p \approx 1$, then it is no longer possible to determine accurately the

value of C_v which is required for resonance, and at still higher frequencies resonance is not even to be attained. An attempt may be made to raise this limiting frequency by putting fewer turns on the Ferroxcube core, so that both L_s and C_p become smaller. There is a limit to what can be done in this direction, however, since by reducing the number of turns the leakage field becomes greater. This will be referred to later.

The measurement is, however, made impossible by other causes before the limiting condition $\omega^2 = 1/L_s C_p$ is reached, either because of the sharply increasing losses in the Ferroxcube ring (tan δ_F no longer small compared with unity), or because the separate determination of the stray capacitance, the accurate knowledge of which becomes increasingly important with rising frequency — as a consequence of a decreasing $C_v{}^0$ — is no longer easily possible.

A further complication arises from the fact that the measured value of tan δ_t, in addition to the quantity tan δ_F needed in the determination of μ_i'', contains also tan δ_D and tan δ_K. These (dielectric and I^2R) losses must therefore be determined separately.

Finally, a further complicating factor is the stray self-inductance of the coil, comprised by the self-inductance of the connecting leads and the self-inductance of the leakage field of the coil; the formulae (3) and (4) are only valid for a toroid which has *no* leakage field.

The errors introduced by the causes summarized here may be minimized in the following way.

The self-capacitance and the dielectric losses in the core may be reduced by inserting a layer of styroflex between the core and the winding (styroflex is a foil of polystyrene, a material of low dielectric constant, which introduces practically no dielectric losses). This layer prevents the lines of electric flux present between two adjacent turns from running through the Ferroxcube (see *fig. 2*). Because of the high values of the real (ε') and the imaginary part (ε'') of the dielectric constant of certain Ferroxcube materials (see I, fig. 10), this would of course result in both a large stray capacitance and large dielectric losses.

The I^2R losses in the copper winding may be kept small by the use of stranded wire, the thickness of the separate wires of which must be matched to the measuring frequency. The fact that there exists for every frequency a wire thickness which is preferably not exceeded, is, as is known, to be ascribed to the presence of the skin-effect. Up to about 10 Mc/s, there is a rule of thumb according

to which the thickness d, in microns, of the separate wires, must be smaller than the wavelength in metres.
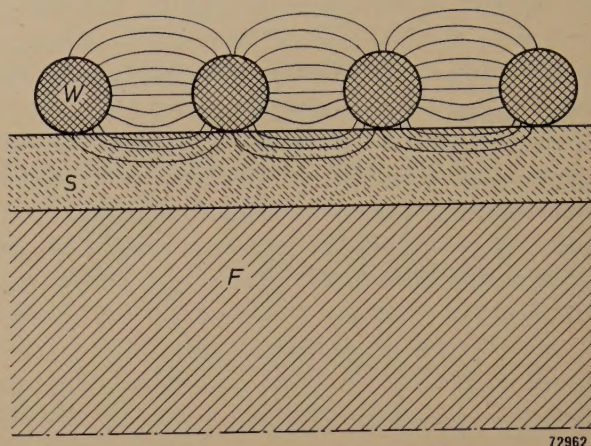

Fig. 2. Influence of a layer of styroflex between the ferromagnetic core F and the turns W. The lines of electric force between two adjacent turns run almost exclusively either in the air or in the styroflex S, which introduces only negligible losses.

Finally, the stray self-inductance of the connecting leads and of the leakage field can be reduced by using short leads lying closely adjacent to each other and by employing a large number of turns. This, however, is at the expense of the measuring range (see above), so that it is necessary to come to a compromise.

The above description of the resonance method is based on the supposition that the measurements are carried out by variation of a measuring capacitance C_v at constant frequency. It is, however, possible to use the analogous method whereby measurements are made by variations of frequency at a constant capacitance C_t. Such a method has the advantage that the stray capacitance need not be determined separately if the loss angle is to be measured, since tan $\delta_t = \Delta f/f_0$; it can, however, lead to difficulties if the permeability and the losses in the frequency range near the measuring frequency depend sharply on the frequency.

Measurements at high frequencies (5 Mc/s-3000 Mc/s)

The method now to be described, for high frequencies (5 Mc/s-3000 Mc/s), is also a resonance method, which, however, no longer uses "lumped" circuit elements. Use is made, rather, of a resonant coaxial line [3]). The special advantage of this method is that no turns have to be wound on the core and

[3]) Regarding the coaxial line, see for example: C. G. A. von Lindern and G. de Vries, Philips tech. Rev. **6**, 240, 1941. For a more extensive treatment see, for example, R.W.P. King, H. R. Mimmo, A. H. Wing, Transmission Lines, Antennas and Waveguides, Mc Graw Hill Book Co., New York, London, 1945.
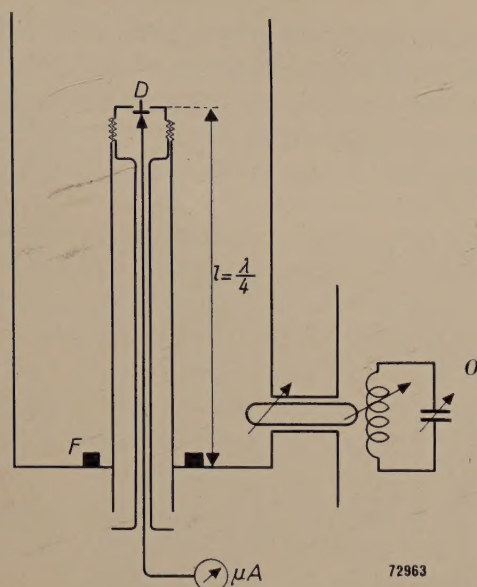
Fig. 3. Coaxial line ($l = \lambda/4$) for the measurement of μ' and μ'' at high frequencies. O oscillator, D detector, coupled to the electric field, F Ferroxcube ring.

that all the inherent sources of error and limitations are eliminated.

The frequency range under consideration must be further divided into two parts. A coaxial $\lambda/4$ resonator for the lowest frequency of this range would be much too long to be used in practice. It is therefore more practical to use an open $\lambda/4$ resonator (see *figs* 3 and *4*) in the frequency range of 100 Mc/s-3000 Mc/s — or, at the highest frequencies, for greater convenience, a $(2n + 1)\ \lambda/4$ resonator — whilst for the range of 5 Mc/s-100 Mc/s a coaxial resonator is used in combination with a "lumped" capacitance which is connected to the upper end of the line (top capacitance) (see *figs* 5 and *6*); a coil may also be connected in series in the circuit. This small change in the set-up has, however, no consequences of a fundamental character.

The measuring equipment is set up as follows. A coaxial line of a certain length l is coupled to an oscillator by means of a magnetic coupling loop. The voltage existing at the upper end of the resonator is determined with the aid of a crystal detector, which is placed inside the inner conductor, at the top. For convenience of measurement it is essential that the couplings between the coaxial resonator and the oscillator and between the detector and the resonator are so weak that the amplitude and frequency of the oscillator are independent of the setting of the resonator, and also that the resonator is not influenced by the detector.

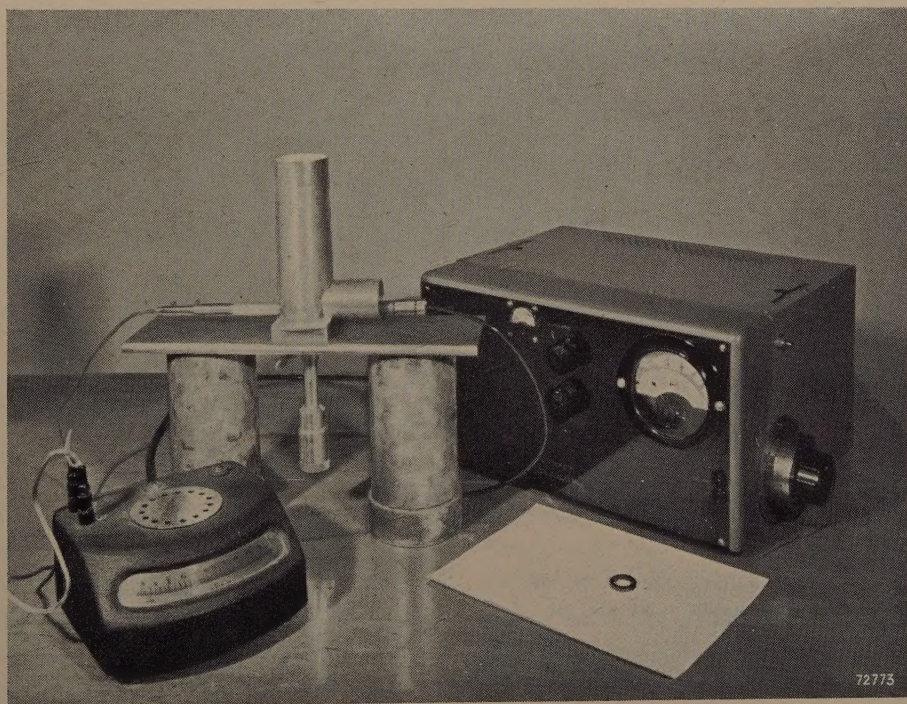The measurement of the real and the imaginary parts of the initial permeability μ_i of Ferroxcube

Fig. 4. Photograph of the equipment shown diagrammatically in fig. 3. At the right, the oscillator, in the centre, a coaxial $\lambda/4$ resonator suitable for frequencies from 500-2000 Mc/s, with adjustment screw underneath for variation of the length. The projecting portion of the resonator at the left is the detector, which, however, different from the position shown in fig. 3, is coupled to the magnetic field. In front of the oscillator is a Ferroxcube ring.
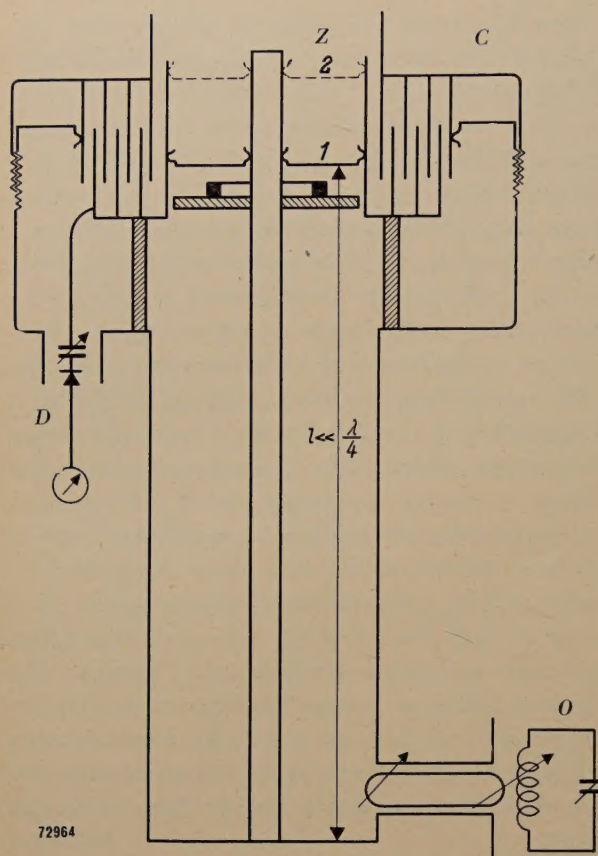
Fig. 5. Coaxial line ($l < \lambda/4$) in combination with a lumped capacitance. O oscillator, D detector, C lumped variable capacitance, Z movable piston in two positions 1 and 2, with Ferroxcube ring underneath.

at a given frequency is now carried out in a series of steps [4]):

1a) Determination of the resonance length l^0 (or, in the case of a line terminated by a capacitor, of the resonance capacitance C^0) of the empty line.

1b) Determination of the difference Δl_0 (ΔC_0) between the two values for the empty line at which the voltage is $1/\sqrt{2}$ times its maximum value. From the resonance width thus obtained, the quality factor Q_0 of the empty line is derived: $Q_0 = l^0/\Delta l^0$ ($C^\circ/2\Delta C_0$).

2a) A ring of Ferroxcube material is introduced into the coaxial line at a point where the electric field strength is practically zero. The length variation δl_F (or alternatively the capacitance variation δC_F) necessary to adjust the voltage at the top end of the resonator to its maximum is now determined.

2b) Determination of the resonance width, expressed as Δl_F, or alternatively ΔC_F, for the line with Ferroxcube ring.

In principle all the data are now available which, together with the dimensions of the ring and the measuring line, are necessary for the determination of the two components of the permeability of the Ferroxcube. The formulae can be simplified, however, if one first measures for a copper ring the quantity δl_K (δC_K) corresponding to the quantity δl_F (δC_F), the copper ring having the same dimensions as the Ferroxcube ring [5]). Because of the skin-effect the magnetic field penetrates only to a very small depth into the copper ring, so that in the frequency range employed the copper ring can, to a close approximation, be regarded as a ring with magnetic permeability $\mu' = 0$.

If the quality factor of the line with Ferroxcube ring is sufficiently high:

$$(l^0 + \delta l_F)/\Delta l_F \quad \text{or} \quad (C^0 + \delta C_F)/2\Delta C_F > 10,$$

and if the relative detuning $\delta l_F/l^0$ or $\delta C_F/C^0$ is small in comparison with unity, then:

$$\mu_i'/\mu_0 - 1 = -\frac{\delta l_F}{\delta l_K}, \quad \text{or} \quad \mu_i'/\mu_0 - 1 = -\frac{\delta C_F}{\delta C_K}. \quad (9)$$

The imaginary part of the permeability is given by:

$$\mu_i''/\mu_0 = \frac{\Delta l_F - \Delta l_0\,(1 + \delta l_F/l^0)^2}{2\delta l_K}$$

$$\text{or} \quad \mu_i''/\mu_0 = \frac{\Delta C_F\,(1 + \delta C_F/C^0)^{-2} - \Delta C_0}{2\delta C_K}. \quad (10)$$

The difficulties limiting the applicability of the resonance method as carried out according to the previous section, are obviated by this coaxial set-up.

The condition that the quality factor of the empty resonator and of the resonator with Ferroxcube ring must be high, still applies because the formulae given are only accurate to the exclusion of terms of the order of $\tan^2 \delta$ and that otherwise the resonance peak is no longer sharp enough for the accurate determination of δl_F (δC_F). This does not mean, however, that only Ferroxcube materials with a low $\tan \delta_F$ may be measured by the coaxial method. The ferromagnetic ring occupies only a small portion of the volume of the coaxial line, so that the quality factor of the line can still be high even in the presence of a ring with high losses.

No stray capacitance is present in the coaxial method, since the Ferroxcube ring is placed in the line at a point where there is no electric field. For the same reason there are no difficulties due to the introduction of dielectric losses.

---

[4]) For the sake of simplicity the description of the case where the frequency of the oscillator is varied will be omitted. The procedure is closely analogous and affords no further insight. Further, the remarks made at the end of the previous section regarding the frequency variation method apply here also.

[5]) H. J. Lindenhovius and J. C. van der Breggen, Philips Res. Rep. **3**, 37, 1948.

The I^2R losses arising from the finite conductivity of the walls of the coaxial line are, of course, present, so that the quality factor of the empty line is not infinitely high. In contrast to the application of the resonance method described earlier for low frequen-

greater than the order of 1% are to be avoided there are a few further stipulations to be complied with to ensure accurate measurements: viz., the relative detuning $\delta l_F / l^0$ must not be too great, since terms of the order of $(\delta l_F / l^0)^2$ are neglected

Fig. 6. Photograph of the equipment shown diagrammatically in fig. 5. At the right, the oscillator, on which is lying an open coaxial $\lambda/4$ line which is used in the range of 250-1000 Mc/s. At the end of the central conductor the electrically coupled detector can be seen. Standing at the left, a coaxial line with variable top capacitance, for frequencies of 5-100 Mc/s. To the left of this line is the electrically coupled detector. The helix in the foreground is the inner conductor of a line, in which the helix serves as lumped inductance (see text).

cies, the I^2R losses in the coaxial method are easily measured and allowed for in the calculations (see formula 10). In the former method the losses in the winding without core cannot be measured in any simple manner, since the distribution of the electromagnetic field is strongly influenced by the presence of the core.

Moreover, there is no stray self-inductance in the coaxial method.

Apart from the previously mentioned condition that the quality factor of the line with Ferroxcube ring may not be smaller than 10 if errors

in the formulae. This condition can always be met either by the use of a longer line, or by introducing a "lumped" inductance in series with the measuring line.

On the other hand the losses and the detuning may not be too small to permit of their sufficiently accurate measurement. In many cases this can be arranged by using a short coaxial line in combination with a large capacitance, and, possibly, by choosing the height of the Ferroxcube ring large.

In the event that a type of Ferroxcube has to be investigated which possesses a high permeability

(e.g. $\mu_i' = 1000\ \mu_0$), the following problem arises. Such a Ferroxcube ring gives rise to a detuning $\delta l_F(\delta C_F)$ 1000 times as great as that needed for a copper ring of the same dimensions. Since satisfactory accuracy of measurement cannot be achieved in this way, the Ferroxcube must in this case be compared with a copper ring of much greater dimensions than the Ferroxcube ring, so that the detuning differ by not more than e.g. a factor 10. In practice such a copper ring is replaced by a movable piston in the upper part of the coaxial line (see fig. 4). The movement of the piston is then equivalent to the insertion or removal of a large copper ring of known dimensions. From the detuning measured after removing the Ferroxcube ring by lowering the piston, the detuning which would be caused by a copper ring with the same dimensions as the Ferroxcube ring can easily be calculated, upon which formulae (9) and (10) again give the components of the permeability.

The only real difficulty which must be borne in mind in the interpretation of results obtained by the coaxial method lies in the **dimensional effects** occurring at these high frequencies, due to the cross-sectional dimensions of the ring being no longer small compared with the wavelength [6]). As a consequence of these dimensional effects, the measured values of the permeability depend on the shape and size of the Ferroxcube ring used in the measurements, so that further corrections must be introduced to derive the material characteristics (independent of the shape) from the measured values. This results, however, in complicated calculations, and demands, moreover, a knowledge of the complex dielectric constant of the material at the frequency employed. For this reason these calculations should be obviated as far as possible by choosing the height of the ring sufficiently small.

Measurements in strong fields

The magnetization curve

The magnetization curve at a given frequency implies here the relation existing between the am-

[6]) See I, p. 193.

plitude H_m of a magnetic field varying sinusoidally with time and the maximum value B_m of the periodically (but in general not sinusoidally) alternating flux density in the ferromagnetic material, the latter being demagnetized before the measurement (see *fig. 7*). We thus deviate slightly from the accepted terminology. The definition given above is only of practical significance for ferromagnetic materials with a high resistivity, since in the case of metallic ferromagnetic materials, the magnetization curve defined in this way would depend on the shape and dimensions of the material being examined.
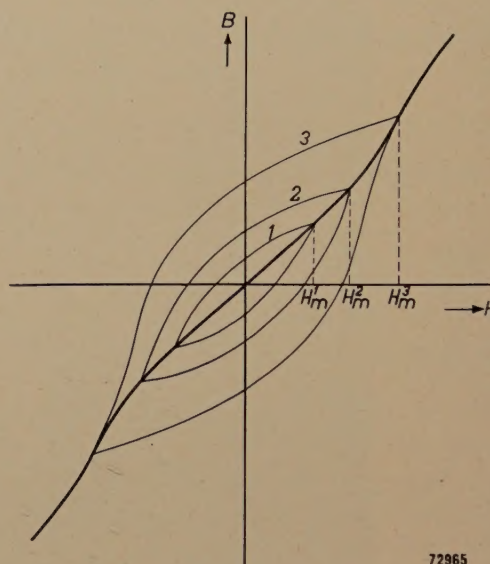
Fig. 7. At low frequencies there is a hysteresis loop for each value of H_m. Three examples are given in the figure. The extremities of the hysteresis loops lie on the heavily drawn line, representing the magnetization curve at high frequencies.

The measurement of the magnetization curve is carried out, schematically, as follows (see *fig. 8*). The primary coil (inductance L_p) of a transformer with a toroidal Ferroxcube core is fed from an oscillator with variable frequency. The primary current (r.m.s. value i_p) supplied by the oscillator and measured by a milliammeter must be as purely sinusoidal as possible. The magnetic field
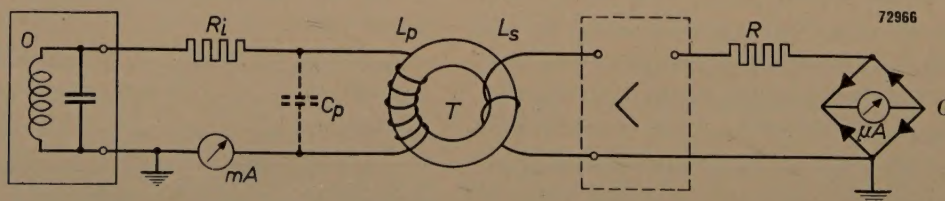

Fig. 8. Diagram of the method for the determination of the magnetization curve. O oscillator, R_i resistance of the primary circuit, L_p primary inductance, C_p stray capacitance. T transformer with toroidal Ferroxcube core, L_s secondary inductance, R resistance of secondary circuit, G full-wave rectifier circuit.

excited in the core by the primary current has a peak value:

$$H_{\mathrm{m}} = \frac{i_{\mathrm{p}} n_{\mathrm{p}} \sqrt{2}}{l}. \quad . \quad . \quad . \quad . \quad (11)$$

In the above relation n_{p} is the number of turns in the primary coil and l is the length of the centre line of the core.

The measurement of the secondary voltage of the transformer is carried out by means of a full-wave rectifier circuit as shown in fig. 8. As a consequence of the full-wave rectification the reading of the microammeter is proportional to the average value of the secondary voltage $E_{\mathrm{s}}(t)$ over a half-cycle, with the initial condition $E_{\mathrm{s}}(0) = 0$:

$$\bar{E} = \frac{\omega}{\pi} \int_{0}^{\frac{\pi}{\omega}} E_{\mathrm{s}}(t)\, \mathrm{d}t. \quad . \quad . \quad . \quad . \quad (12)$$

$E_{\mathrm{s}}(t)$ is related to the derivative of the magnetic flux Φ as follows:

$$E_{\mathrm{s}}(t) = -\frac{\mathrm{d}\Phi}{\mathrm{d}t} = -n_{\mathrm{s}}O\frac{\mathrm{d}B}{\mathrm{d}t},$$

in which n_{s} is the number of secondary turns and O the cross-sectional area of the core. By substitution in (12) we find:

$$\bar{E} = -\frac{\omega}{\pi} n_{\mathrm{s}}O\left[B\left(\frac{\pi}{\omega}\right) - B(0) \right] = 2\frac{\omega}{\pi} n_{\mathrm{s}}O\,B_{\mathrm{m}},$$

and thus:

$$B_{\mathrm{m}} = \frac{\pi\,\bar{E}}{2\omega\,n_{\mathrm{s}}\,O}. \quad . \quad . \quad . \quad . \quad (13)$$

The limitations of and sources of error in the method described are as follows.

The value read from the milliammeter (see fig. 8) is not equal to the r.m.s. value of the primary current i_{p}, since there is always a stray capacitance present in parallel with the primary winding. If we stipulate that the current flowing through the stray capacitance is less than 1% of the current flowing through L_{p}, the following condition must be satisfied:

$$\omega^2 L_{\mathrm{p}} C_{\mathrm{p}} \leq 10^{-2}. \quad . \quad . \quad . \quad . \quad (14)$$

Owing to the non-linear relationship between B and H at the field strength under consideration, the flux in the core will no longer be purely sinusoidal, but will contain, inter alia, a component varying with time in proportion to $\sin 3\omega t$ (third harmonic). Thus the voltage across the primary inductance will contain, apart from a component V_{p1}, which varies with the angular velocity ω, a further component V_{p3}

which varies with the angular velocity 3ω. To keep the primary current approximately sinusoidal, we must stipulate that the value of the current i_{p3} caused by the above-mentioned V_{p3} is smaller than $0.01\,i_{\mathrm{p1}}$, i_{p1} being the desired current component alternating with angular velocity ω. It can be assumed that for most cases the e.m.f. due to the third harmonic is smaller than $0.1\,V_{\mathrm{p1}} = 0.1\,i_{\mathrm{p1}}\omega L_{\mathrm{p1}}$. From this it follows that i_{p3} is smaller than

$$\left| \frac{0.1\,i_{\mathrm{p1}}\omega L_{\mathrm{p1}}}{R_{\mathrm{i}} + \mathrm{j}\,3\omega L_{\mathrm{p3}}} \right|,$$

and, according to our stipulation, this must also be smaller than $0.01\,i_{\mathrm{p1}}$. In this expression R_{i} is the resistance in the circuit in series with the primary coil, which is practically the same as the total external impedance for the third harmonic. If this condition is further developed, the conclusion is reached that, if L_{p3} is assumed not to differ sharply from L_{p1}, then:

$$R_{\mathrm{i}} \geq 9\omega L_{\mathrm{p}}. \quad . \quad . \quad . \quad . \quad (15)$$

The branch containing the stray capacitance C_{p} must also, of course, have a sufficiently large impedance for i_{p3}. From this arises the condition:

$$13 \times 3\omega L_{\mathrm{p}} \leq \frac{1}{3\omega C_{\mathrm{p}}},$$

which is practically the same as the condition (14).

The maximum field strength which can be employed for measurements is limited both by the conditions (11) and (14), and by the maximum current value which the oscillator can supply. Thus, for a given frequency $\omega/2\pi$ and a given stray capacitance C_{p}, L_{p} and hence the number of turns n_{p} is limited.

At high frequencies and high field strengths difficulties may also be experienced by the large amount of heat developed in the core. This latter, coupled with the low thermal conductivity of the Ferroxcube material, makes it essential that all measurements are carried out quickly and that a long period must elapse between two measurements.

Losses at high values of flux density

As was amply shown earlier in I, various physical processes contribute to the losses in the range of high values of the flux density. These various contributions cannot easily be separated in a general way. In this range of high flux densities it is therefore only possible to investigate the magnitude of the total losses occurring in a unit volume of a Ferroxcube

core when a purely sinusoidal, alternating magnetic field of large amplitude is present.

There are two different methods available for determining this quantity. In the first method the heat developed in the Ferroxcube core by the alternating electromagnetic field is measured directly in a calorimeter. The second method is similar to the coaxial method described in a previous section.

a) Calorimetric method

In the calorimetric method a winding on a ring-shaped core of Ferroxcube is again employed. The coil with core is placed in a calorimeter, and the coil is supplied with a sinusoidal current. The total quantity of heat developed in a certain time due to the energy dissipation in the core can now be determined from the temperature rise in the calorimeter. This method offers the advantage that one can in this way determine with certainty *all* the losses arising in the core due to the electromagnetic field. One measures thus not only all types of ferromagnetic losses but also the dielectric losses. This appears to be a useful method for flux densities exceeding 50×10^{-4} Wb/m² and in a frequency range between 50 kc/s and 1 Mc/s. The stipulation that the frequency may not be too low and the flux density not too small is occasioned by the sensitivity of the calorimeter; the heat developed per unit time may not be too small. That the calorimetric method is not suitable for frequencies over a certain value is a consequence of the self-capacitance C_p of the winding on the core, mentioned repeatedly above. This results in the measured value of the current through the winding not being the true value, so that an exact determination of the field strength is no longer possible.

Apart from these limitations, a further disadvantage of the calorimetric method is that the measurements require much time. This method is thus not suitable for routine investigations.

b) The coaxial method

The limitations of the calorimetric method are avoided in the coaxial method, although this in turn is subject to other limitations. The latter method can be satisfactorily applied for flux densities lying below 100×10^{-4} Wb/m². Hence measurements can also be carried out in the range not encompassed by the calorimetric method (below 50×10^{-4} Wb/m²). The frequency range of the measuring apparatus made in the Philips laboratory in Eindhoven lies between 50 kc/s and 10 Mc/s.

As we have already mentioned, the coaxial method described here is similar to that already discussed on pages 248-252, and which was intended for use at very small values of flux density. For measurements at high values of flux density, however, the power of the oscillator must be considerably greater. Because of the low frequency, the measuring circuit always contains a "lumped" inductance and capacitance.

As with the coaxial method for measurements at very low values of flux density, the change in the resonance capacitance and the change in the width of the resonance curve due to the insertion of the Ferroxcube ring into the resonator, are determined in this case also. This amounts to the determination of the real (μ') and the imaginary (μ'') components of the magnetic permeability (μ). However, in the introduction it was shown that the values μ' and μ'' become meaningless at high values of flux density. The contradiction between these two statements is only apparent, as we shall now see. The two measured quantities μ' and μ'' are no longer the real and the complex components of a permeability defined by a relation $B = \mu H$. Rather must this relation be replaced by one of the form:

$$B = (\mu_i + \nu H_m) H \pm \nu (H_m{}^2 - H^2), \qquad (16)$$

in which H_m is the maximum field strength. The $+$ and $-$ signs must be used for the upper and lower branches of the hysteresis loop respectively; ν is the Rayleigh constant. By the coaxial method, therefore, one thus measures the components of the first term of the right-hand side of (16). The error involved is not easily estimated. The complexity and confusion of this situation (and the resulting limited accuracy of the results) is one of the disadvantages of this method. In general, one can say that not the total losses arising in the Ferroxcube ring are determined, but principally the losses corresponding to that part of the magnetic flux density having the same periodicity as the magnetic field. This is associated with the fact that the peak value of the voltage across the resonator is measured by this method. This value is mainly dependent on the flux density component with the fundamental frequency. The voltages due to the higher harmonics, which add with an unknown phase to the voltage of the fundamental frequency, are small since there is no resonance for the higher harmonics.

For flux densities up to about 50×10^{-4} Wb/m² this has no unfavourable consequences of any importance in practice: comparison with loss measurements by the calorimetric method shows that errors made with the coaxial method in the range of the

flux density mentioned are in general small. If, however, reliable results in the range above $50 \cdot 10^{-4}$ Wb/m² are desired, then resort must be taken to the elaborate calorimetric method.

Distorsion

From the above-mentioned relation (16) between B and H it follows that, at large values of the maximum field strength H_m, deviations from the linear relationship between current and voltage appear. If, thus, a purely sinusoidal current of angular velocity ω flows through the primary winding of a transformer, a voltage is produced across the secondary winding which may be described by the following series [7]:

$$V = V_1 \sin \omega t + V_3 \sin 3\omega t + V_5 \sin 5\omega t + \ldots \quad (17)$$

The distortion is now defined by:

$$D = \sqrt{\frac{V_3^2 + V_5^2 + \cdots}{V_1^2}}.$$

In general, however, the higher harmonics V_5 etc. may be neglected, so that by approximation:

$$D \approx \frac{V_3}{V_1}. \quad \ldots \ldots \ldots \quad (18)$$

The most direct method of measuring the distortion is the following. The voltage across the secondary winding of a transformer is measured by means of a selective voltmeter. In this way the values V_1 and V_3 are at once determined.

More usual, but, as we shall see, not to be used without caution, is another procedure which we shall describe more fully.

For sufficiently weak fields there is a simple relation between the distortion V_3/V_1, the angular velocity ω of the fundamental wave, the inductance L of the (primary) coil and the hysteresis resistance R_H [8]:

$$\frac{V_3}{V_1} = \frac{0.6 \, R_H}{\omega L}. \quad \ldots \ldots \ldots \quad (19)$$

The existence of this relationship introduces the possibility of determining the distortion by measurement of the hysteresis resistance.

The hysteresis resistance, which represents the loss caused by hysteresis in a coil with a ferromagnetic core, is a quantity depending on the maximum field strength. If we assume that the loss due to hysteresis is the only type of loss depending on

the field strength, which in general is certainly not the case [9]), then the hysteresis resistance R_H may be found from a graph in which the total resistance R_t is plotted as a function of the maximum field strength H_m according to the relation:

$$R_H = R_t - R_0, \quad \ldots \ldots \quad (20)$$

in which R_0 is the part of the resistance independent of the field strength. At "low" frequencies R_t may be measured, for example, with the aid of a Maxwell bridge [10]).

With the same conditions as for (19), it can be deduced that, for a given value of H_m, R_H increases proportionally to the frequency. Measurements on Ferroxcube materials have shown, however, that above a certain frequency range (depending on the material) the value of the hysteresis resistance found according to (20) is greater and increases more sharply with frequency than is to be expected from the results of distortion measurements with the aid of a selective voltmeter. This indicates that at high frequencies another loss mechanism occurs which also depends on the maximum field strength, so that the relation (20) can no longer be used to determine, from the measured value R_t, the resistance R_H, which is associated only with hysteresis phenomena. This is clearly seen in *fig. 9.*
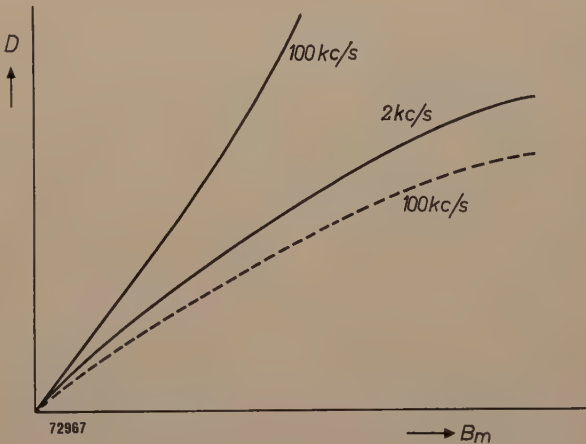
Fig. 9. Distortion D in Ferroxcube as a function of the maximum flux density B_m, at 2 kc/s and at 100 kc/s (schematic). The full line for 100 kc/s gives the distortion as would be derived from the apparent hysteresis resistance. The broken line gives the results of measurements with a selective voltmeter. At 2 kc/s the results by both methods are identical.

This gives the distortion schematically as a function of the maximum flux density for two different frequencies. The full line for 100 kc/s gives approximately the distortion to be found by calculation

---

[7] The fact that no even harmonics appear in this series is due to the symmetry of the hysteresis loop about the origin of the co-ordinates for B and H.

[8] E. Petersen, Bell Syst. tech. J. **7**, 762, 1928.

[9] For a full discussion of this hypothesis see I.

[10] See for example D. Polder, Proc. I.E.E. **97**, 246, 1950.

from the "apparent" hysteresis resistance according to formulae (20) and (19); the broken line for 100 kc/s gives approximately the values found by the method using the selective voltmeter. Whilst the results found by the two methods agree for very low frequencies (see the curve for 2 kc/s), one sees that at the higher frequencies a marked discrepancy appears. The distortion can thus not be determined at high frequencies by use of the relations (20) and (19), and recourse has to be made to the rather less simple method already mentioned, using a selective voltmeter.

———

Summary. For the measurement of the permeability and the losses of Ferroxcube materials in weak fields, a resonance method is applied in which the measuring circuit consists of either lumped network elements (for a frequency range of about 50 kc/s to 10 Mc/s), or of a coaxial line with or without a lumped inductance or capacitance (for frequencies in the range between 5 Mc/s and 3000 Mc/s). The sources of error and limitations of both methods are amply described. In strong fields a determination of the magnetization curve replaces the permeability measurement. This is carried out with the aid of a full-wave rectifier circuit in which the secondary voltage of a transformer with Ferroxcube core is measured. Two methods are available for the measurement of losses in strong fields. In the first method the quantity of heat generated in a Ferroxcube ring placed in a sinusoidally alternating magnetic field is measured in a calorimeter. This method is suitable for flux densities above 50×10^{-4} Wb/m^2 and frequencies below 1 Mc/s. A disadvantage is that a measurement is rather elaborate. For smaller flux densities and at higher frequencies use can again be made of a coaxial line. As a result of the distortion inherent in this method, however, not the total losses but only those caused by the fundamental frequency are measured. This is no disadvantage below 50×10^{-4} Wb/m^2. Finally, some remarks are made on the measurement of the distortion. At very low frequencies the distortion may be determined from measurements of that part of the resistance which depends on the maximum field strength, whereas at high frequencies the distortion must be measured directly with the aid of a selective voltmeter.

A DIRECT READING PRECISION POLAROGRAPH

by H. A. DELL *) and C. H. R. GENTRY **).

545.33 : 621.317.755

For the last few years it has been usual in metallurgical investigations to measure the concentration of certain metal ions with the aid of a polarograph. An objection against the use of this instrument is that the taking of a polarogram and the deriving of the desired results take up much time. The polarograph described in the following removes this objection as the results can be read directly from the instrument.

Introduction

There are various types of electrical measuring apparatus in use in chemical analysis at the present time. An example is the polarograph, which is used extensively in metallurgical investigations. With this instrument the current which flows when a particular voltage is applied between two electrodes located in the liquid to be analysed can be measured. From the form of the curve giving the current as a function of voltage, the so-called polarogram, the presence of certain metal ions in a solution can be investigated qualitatively and quantitatively.

The anode may be a mercury pool, a calomel or other electrode, non-polarizable under the conditions to be studied. The cathode consists of a small drop of mercury which is suspended from a capillary tube.

As the currents to be measured are of the order of a few microamperes, a galvanometer is usually employed, making the apparatus rather delicate. As far back as 1939, a description was given in this periodical of a method whereby the galvanometer was replaced by a cathode ray oscillograph or a measuring bridge, giving not only a more robust set-up but also an appreciable shortening in the time required for the analysis of a given liquid [1]. For a qualitative analysis it is in this case no longer necessary to take a full polarogram and to measure it afterwards; this is replaced by an indication on the cathode ray tube and a reading of a calibrated scale.

In the following we shall give a description of an instrument which likewise uses a cathode ray tube as indicator, but which makes possible not only qualitative but also quantitative analysis. With the polarographs usually employed conclusions about the composition of the liquid to be analysed can only be drawn after plotting a complete polaro-gram. With the instrument to be described, however, the concentration of certain metal ions can be deduced from the difference of two readings, resulting in a considerable saving of time. Moreover, the measurements are as exact as or even more exact than is usually the case in polarography [2].

The polarograph in question is shown in *fig. 1*. Before describing this apparatus, we shall first recapitulate a few particulars concerning electrolysis with the mercury-drop electrode. (See also the article referred to in footnote [1]).

Electrolysis with a mercury-drop electrode

If one applies, between two electrodes immersed in a metallic salt solution, a D.C. voltage which is gradually increased from zero, no appreciable immediate flow of current is, as a rule, to be observed. This is due to the fact that a metal ion requires a certain voltage to discharge it. This voltage differs for ions of different types. Only at a voltage that is sufficiently high can an ion of the element which has the lowest deposition voltage join with an electron from the cathode to form a metal atom. If this voltage is reached the electrons which are drawn from the cathode are replenished by the voltage source, so that an electric current is produced. If the solution is not too concentrated, and if a cathode of small surface area is used, then with a further increase of voltage the position is soon reached at which every metal ion arriving at the cathode is immediately discharged. The current then depends on the ion concentration, the surface area of the cathode and the speed with which the ions migrate to the cathode. The speed of migration of the ions considered is independent of the voltage, provided that there exists in the solution

*) Mullard Research Laboratory, Salfords, England.
**) Mullard Material Research Laboratory, Mitcham, England.
[1] J. Boeke and H. van Suchtelen, Rapid chemical analysis with the mercury dropping electrode and an oscillograph or measuring bridge as indicator, Philips tech. Rev. **4**, 231-236, 1939.

[2] A description of the instrument has already been given in two earlier publications: C. H. R. Gentry and D. Newson, Metallurgia **41**, 107-111, 1949 (Dec.); H. A. Dell and C. H. R. Gentry, Electronic Eng. **28**, 19-21, 1952 (Jan.).

Fig. 1. The direct reading precision polarograph. On the left is a thermostat in which is placed the electrolytic cell with the solution under investigation and the mercury drop electrode.

an excess of ions having a higher deposition voltage. If the current is now plotted as a function of the voltage, a curve (polarogram) is obtained similar to that shown in *fig. 2*.
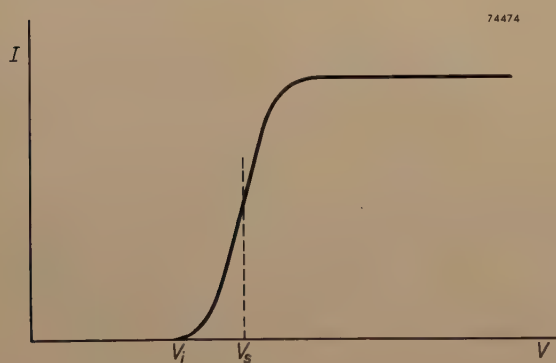

Fig. 2. Simplified representation of part of a polarogram. (The charging current of the drops is not shown.) V_i is the potential at which a current I just begins to flow in the solution, and V_s the half-wave potential.

The half-wave potential V_s is characteristic for the kind of ions considered. If various types of ions are present in the solution, current steps appear at different values of voltage. A polarogram will thus take the shape of *fig. 3*. As the magnitude of the current steps is proportional to the concen-

tration of the various ions, one can determine the latter quantity by measuring the former.

By making the cathode very small a danger is introduced that the surface will become contaminated quickly by deposition of metal. This difficulty is overcome by using as cathode a small drop of mercury hanging from a capillary tube. By supplying mercury to the tube, the drop is caused to fall off periodically, at intervals of a few seconds, thus regularly renewing the cathode surface. The falling and reforming of the mercury droplets, however, render the measurement more difficult. As the surface area of the cathode continually alters, the

Fig. 3. Shape of a polarogram in the presence of various types of metal ions in the solution being examined.

current also changes during the life of each drop, so that for a given voltage the current varies as a function of time as shown in *fig. 4*. When the drop is very small the current is small, whilst as the drop increases in size so also does the current increase, as in curve *AB*. When the drop falls the current drops suddenly as shown by the line *BC*. It can be shown that the current during the life of each drop is proportional to the one-sixth power of the time.

In conventional polarographs a galvanometer is used with a very high inertia in order to measure the average value of the current. Since, however, the drops fall at intervals of 3 to 4 seconds, it is not possible completely to damp the oscillations of the galvanometer; to achieve this the damping would have to be so great that the form of the resulting curve would be influenced. It is therefore better only to measure the current at a certain
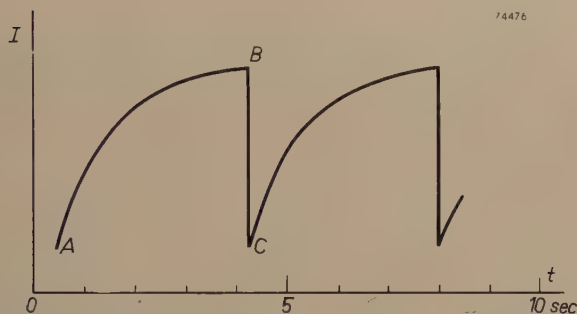

Fig. 4. Current variation in the electrolytic cell as a function of time, at constant voltage. As the mercury drop increases in size, the current rises as shown by the curve *AB*; when the drop falls, the current drops as shown by the line *BC*.

moment during the life of each drop. The most suitable time is the moment just prior to the fall of the drop, for the following reasons:

1. When a drop is detached from the cathode, the equilibrium conditions in the neighbourhood are violently upset and it is thus very difficult to interpret precisely the current early in the life of the drops.

2. The current changes most slowly at the end of the life of the drops, and consequently it is easiest to measure the current at this moment.

In the instrument to be described, therefore, the current is measured at the moments immediately prior to the falling off of the drops.

Use of an oscillograph for measurements with a polarograph

It is desirable to make up the circuit in such a way that the oscillograph is used as a zero voltage indicator, making a calibration of the instrument unnecessary. A circuit which can be used for this purpose is shown in *fig. 5*. By means of the variable resistor R_2 a definite voltage can be applied across the potentiometer R_1, the voltage V_1 thereafter being read on a calibrated scale on R_1. (The resistance of

Fig. 5. A circuit whereby the current in the electrolytic cell Z can be measured by means of a zero voltage method. If no voltage exists between P and Q the current in Z may be read from a calibrated scale on R_5.

R_1 must be so small that the influence of the current in the electrolytic cell Z on the voltage distribution along R_1 can be neglected.) A resistor R_3 is connected in series with Z. This resistor is connected to the sliding contact of a potentiometer R_5, which in series with the resistors R_4 and R_6 is connected across the same voltage as R_1. The value of R_3 must be large compared with R_5 and R_6, so that the influence of the current in R_3 on the voltage distribution across R_5 becomes negligible. If now a voltmeter is connected between the points P and Q, and the slider of R_5 so adjusted that no voltage appears between these points, then the voltage across Z is equal to V_1 less a fixed amount, namely the voltage on $R_5 + R_6$. During the life of a drop the current in Z and R_3 changes, and this is also the case with the voltage between P and Q. At the moment that no voltage exists between these points the current in Z and R_3 is equal to the voltage across the upper part of R_5 divided by R_3. It is therefore possible to provide R_5 with a calibrated current scale which is valid when no voltage is present between P and Q. In this way the current in Z is indeed measured on a zero voltage basis.

In order to employ a cathode ray oscillograph as a zero voltage indicator, the points P and Q are connected to the vertical deflecting plates via separate two-stage amplifiers. In the lead from P to one of these amplifiers a resistor R_7 is introduced (*fig. 6*), and a high speed relay X which is connected to an alternating voltage of 50 c/s connects and disconnects the input terminals of the amplifiers 100 times per second. When now a voltage of saw-tooth waveform is applied to the horizontal deflecting plates of the cathode ray tube, a figure such as that

shown in *fig. 7* appears on the screen. The straight line *p* corresponds to zero voltage and the curve *q* represents the voltage between *P* and *Q* as a function of time.
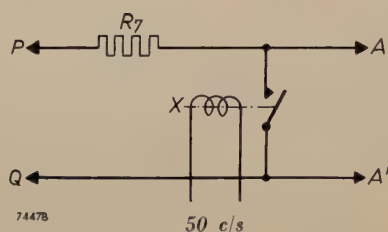

Fig. 6. Circuit permitting the use of a cathode ray tube as zero voltage indicator between points *P* and *Q* (fig. 5). Each of the points *A* and *A'* is connected to one of the vertical deflecting plates of the cathode ray tube via an amplifier. By means of a high speed relay *X*, the points *A* and *A'* are connected and disconnected 100 times per second.

Thus, during measurement, the potentiometer R_5 is so adjusted that the upper tips of the curve *q* just coincide with the line *p*. In this case the voltage between *P* and *Q* is zero at the moments just before the detachment of the drops. Thus the current which flows at these moments in the cell *Z* can be read on R_5. This operation is rendered difficult, however, by the fact that the time interval at which the mercury drops fall is quite large, i.e. 1-4 seconds. The adjustment may be facilitated in two ways. Firstly use of a timebase may be dispensed with, so that two dots appear on the screen, one stationary and the other moving up and down. The slider of the potentiometer R_5 is then so adjusted that the moving point just reaches the stationary one.
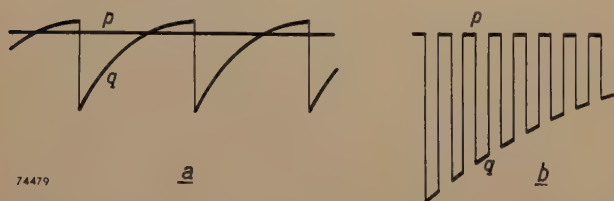

Fig. 7. *a*) Figure produced on the screen of the cathode ray tube by the use of the circuits of figs. 5 and 6. The line *p* corresponds to zero voltage and the curve *q* represents the voltage between *P* and *Q* as a function of time. *b*) Enlargement of part of (*a*). The fluorescent spot traces portions of the lines *p* and *q* alternately.

According to another method the timebase may be synchronised with the falling off of the drops, so that a s t a n d i n g figure preferably consisting of only one period of the current curve appears on the screen (*fig. 8*). To achieve this synchronisation, use may be made of the fact that at the moment of detachment of each drop a voltage pulse of about $1/_4$ V appears across the resistor R_3. It now becomes

simple, in practice, to adjust the top of the curve *q* to coincide with the straight line *p*, particularly when use is made of a tube with a long persistence screen.

The point or the line representing zero input voltage must be very stable to permit of an accurate reading. In order to make the line *p* (figs. 7 and 8) practically rectilinear, or the null-point stationary, it is necessary to use coupling elements with a very large time constant in the amplifier. As a result difficulties might arise due to the long recovery time after an accidental overload. To avoid this disadvantage, use is made of D.C. amplifiers in the present instrument.
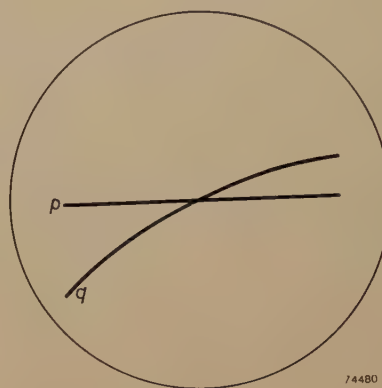

Fig. 8. By synchronisation of the time base with the growth and falling off of the drops, it can be arranged that only one period of the curve *q* appears on the cathode ray tube screen.

The tangent slope control

As already mentioned, for a quantitative measurement not only the half-wave voltages must be measured but also the m a g n i t u d e of the current steps. If a polarogram were to have the form shown in figs. 2 and 3, this would be very simple. One would only have to measure the current at two voltages, the one a little lower and the other a little higher than the half-wave potential. In actual fact, however, the form of a polarogram differs from that shown in figures 2 and 3 in that the flat portions have in reality a slight slope. Thus, in the neighbourhood of a current step, a polarogram takes the form shown in *fig. 9*. The reason for this lies in the fact that each newly formed droplet becomes charged, the charging current being about proportional to the applied voltage. If one now measures the current at either side of the current step, e.g. at voltages *V'* and *V''*, then a value will be found for the current step as represented by I_1 in fig. 9. Actually, the size of the current step which is truly proportional to the concentration of the metal ions concerned is equal to I_2. One can of course determine this value

by taking a full polarogram and drawing in the tangents AB and CD. This method which is in fact usually employed, is naturally a very time-consuming procedure. For this reason the circuitry
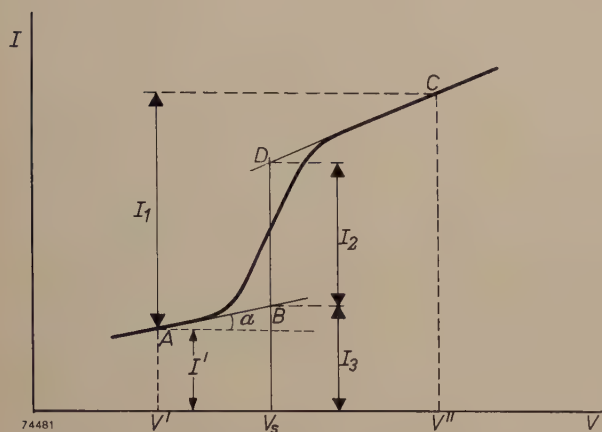

Fig. 9. Due to the charging current of the drops the straight portions of a polarogram show a certain slope. By the use of the polarograph described in this article the current step I_2 can be determined from the difference between two readings I_3 and I_2+I_3.

of the polarograph described here has been extended in such a way that this graphical construction can be simulated electrically. In this way a "direct reading" instrument is obtained.

The modified circuit in which this refinement is introduced is given in *fig. 10*. In this arrangement two variable resistors R_7 and R_8 are connected in series with the potentiometer R_1, the sliders of these two new resistors being coupled in such a
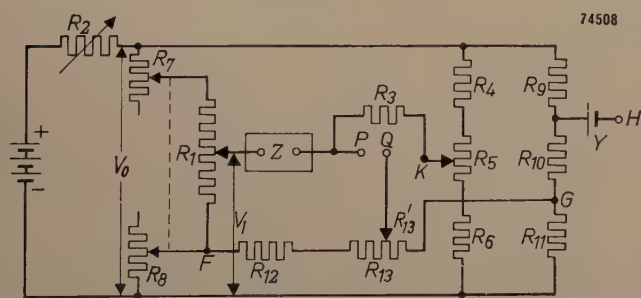

Fig. 10. Polarograph circuit by means of which the charging current of the drops can be compensated. Z electrolytic cell, Y standard cell with the help of which the voltage V_0 may be accurately adjusted to a given fixed value.

way that the total resistance $R_7+R_1+R_8$ remains constant on variation of R_7,R_8. In addition a further potentiometer is introduced, comprising the resistors R_9, R_{10}, and R_{11}. The value of the resistors

is so chosen that the voltage at point F is the same as that at point G, when $R_7 = R_8$. An extra potential divider is connected between these points in the shape of two resistors R_{12} and R_{13}. These latter are of a sufficiently high value to ensure that their influence on the voltage distribution along R_9, R_{10} and R_{11} and along R_7, R_1, and R_8 can be neglected. The point shown in fig. 5 as Q is now connected to the slider of R_{13}.

When this slider is moved to the extreme right the voltage of Q does not change if V_1 is altered by variation of R_7,R_8. The calibration of R_5 has been carried out at this position of R_{13}, so that the current read on R_5 corresponds to the current in the electrolytic cell Z (provided the latter potentiometer is adjusted on the position where no voltage difference exists between P and Q). If $R_7 = R_8$, so that, as already mentioned, the voltage between the points F and G is zero, the moving to the left of the slider of R_{13} has no influence on this situation, since the voltage on Q does not change in this case. If however $R_7 \neq R_8$, so that the voltage of F is not equal to the voltage of G, the position of R_5 at which the voltage between P and Q is zero just before the detachment of the drops, depends on the position of R_{13}.

The procedure in measuring a current step is now as follows: After setting the slider of R_1 in the position where the voltage on the cell Z is equal to the half-wave potential V_s of the element to be determined (keeping $R_7 = R_8$), a change of voltage is introduced by means of R_7,R_8, the voltage on Z becoming for example, equal to V'. R_5 and R_{13} are now adjusted so that at the moment before detachment no voltage appears between P and Q, the setting of these potentiometers being so chosen that for small variations of R_7,R_8 the potential between P and Q remains zero. After a few trials one soon succeeds in this. In this case the variations of the voltages at the points P and Q at small changes of R_7,R_8 are equal. The current which is now read on the calibrated scale on R_5 is not equal to the real value of the current (the calibration having been carried out with the slider of R_{13} moved completely to the right). It can be shown (see appendix) that at the positions of R_5 and R_{13} mentioned, the current read on R_5 is equal to the value which is indicated by I_3 in fig. 9.

When, now, the voltage on the cell is adjusted by means of R_7,R_8 to a value which lies on the other side of V_s, e.g. V'', the value $I_2 + I_3$ can be measured in the same way. The difference of these readings yields the magnitude of the current step I_2.

The complete apparatus

In the final form of the instrument, the resistor R_3 can be changed in five steps. Currents up to 100 microamperes can be measured to an accuracy of 0.1 microampere, differences of 0.01 microampere being still visible. The resistors are so chosen that the voltage applied to the electrolytic cell can be varied between 3.0 V in one direction and 0.3 V in the other direction, which is quite adequate for nearly all ion concentrations to be measured.

For the accurate adjustment of the voltage V_0 to the value at which R_1 and R_5 are calibrated, the voltage across R_{10} is compared with that of a standard cell Y. This may be done in a simple way with the oscilloscope which is already present. For this purpose the amplifiers which during the measurement connect the points P and Q to the deflection plates of the cathode ray tube can be connected to the points which are indicated by H and G in fig. 10.

It appears to be very important to keep the temperature of the solution to be investigated constant. For that reason the electrolytic cell is placed in a thermostat, keeping the temperature constant within 0.05 °C.

The accuracy with which the concentration of certain metal ions can be measured with the instrument described amounts to 0.3 per cent, which compares favourably with the 1 per cent obtainable with existing commercial instruments.

Appendix: Calculation concerning the tangent slope control

We shall denote the voltages between the lowest line in fig. 10 and the points F, P, Q, K and G by V_F, V_P, etc.

The calibration of the scale of R_5 is carried out with $V_Q = V_P = V_F = V_G$, so that at every position of the slider of R_5 the relation between V_K and the value I_{Cal} of the cell current as shown on the calibrated scale is

$$V_K + I_{Cal}R_3 = V_G. \qquad (1)$$

The value of I_{Cal} so obtained is thus only equal to the true value I of the cell current if $V_Q = V_G$. If $V_F \neq V_G$ and the slider of R_{13} is not positioned completely to the right, then this condition is not fulfilled.

In carrying out a measurement V_1 is first so adjusted that, whilst $V_Q = V_P = V_F = V_G$, the cell voltage V is equal to the half-wave potential V_s. From fig. 10 we read that in this case the following holds:

$$V_1 - V_F = V_s. \qquad (2)$$

Maintaining the relationship (2), a change is now made in V_F. We now call the cell current and cell voltage I' and V' respectively (see fig. 9), whilst the slope of the tangent at the point under consideration (A) on the polarogram is indicated by a.

The sliders of R_5 and R_{13} are next so adjusted that the following relationships hold:

$$V_P = V_Q, \qquad (3)$$

$$\frac{\partial V_P}{\partial V_F} = \frac{\partial V_Q}{\partial V_F} \qquad (4)$$

We shall now show that an adjustment of R_5 is thereby reached at which V_K has such a value that the value of I_{Cal} obtained from (1) is equal to the current indicated in fig. 9 by I_3.

If we consider first the branch R_{12}-R_{13} we can write for V_Q:

$$V_Q = V_G + (V_F - V_G)\frac{R'_{13}}{R_{12} + R_{13}}, \qquad (5)$$

thus,

$$\frac{\partial V_Q}{\partial V_F} = \frac{R'_{13}}{R_{12} + R_{13}}. \qquad (6)$$

For V_P, according to fig. 10, we can write.

$$V_P = V_K + I'R_3 = V_1 - V'. \qquad (7)$$

Since a variation of V_F causes an equally great variation in V_1, $\partial V_P/\partial V_F$ is equal to $\partial V_P/\partial V_1$. Considering now the branch Z-R_3 and bearing in mind that for voltage variations the cell Z represents a resistance $\cot a$, then according to fig. 10 the following applies:

$$\frac{\partial V_P}{\partial V_F} = \frac{R_3}{R_3 + \cot a}. \qquad (8)$$

To satisfy (3), V_K and R'_{13} must be so adjusted, according to (5) and (7), that the following equation is satisfied:

$$V_K = V_G + (V_F - V_G)\frac{R'_{13}}{R_{12} + R_{13}} - I'R_3. \qquad (9)$$

At the same time, to satisfy (4), R'_{13} according to (6) and (8) must be equal to the value derived from

$$\frac{R'_{13}}{R_{12} + R_{13}} = \frac{R_3}{R_3 + \cot a} \qquad (10)$$

(V_K plays no role in this).

We find now for the value of I_{Cal} corresponding to V_K, from (1), (9), and (10):

$$I_{Cal} = I' + (V_G - V_F)\frac{1}{R_3 + \cot a}. \qquad (11)$$

Since it follows from (3), (5), (7) and (10) that:

$$V_s - V' = (V_G - V_F)\frac{\cot a}{R_3 + \cot a},$$

we can write for (11):

$$I_{Cal} = I' + (V_s - V')\tan a = I_3.$$

Summary. In this article a polarograph is described which is direct reading, so that in making a quantitative analysis it is not necessary to plot a complete polarogram. The concentration of certain metal ions in the solution to be analysed can be deduced from the difference of two readings on the instrument. As cathode, use is made of a mercury drop which is renewed every 1 to 4 seconds. The current flowing in the solution is measured at the moments just prior to the detachment of the drops. As an indicating instrument a cathode ray oscilloscope is used. The possibility of reading the value of the current steps directly on the instrument is obtained by use of a circuit with which the graphical construction on the polarogram is simulated electrically.
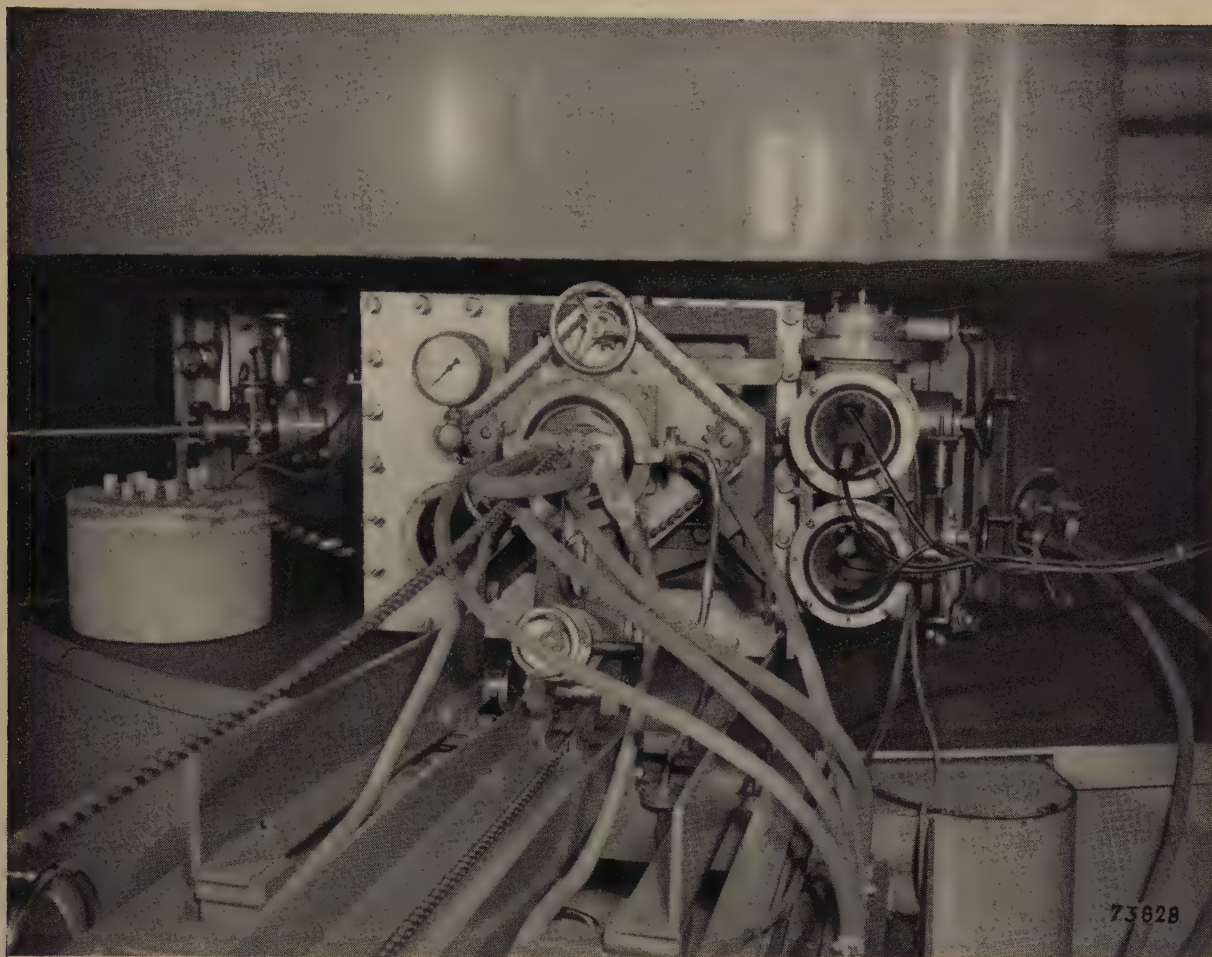
THE SYNCHROCYCLOTRON AT AMSTERDAM

IV. DETAILS OF CONSTRUCTION AND ANCILLARY EQUIPMENT

by F. A. HEYN *) and J. J. BURGERJON **).   621.384.61

The Philips synchrocyclotron at Amsterdam has now been in continual use for three years as a tool for nuclear-physics research and the production of radio-active isotopes. During these three years many other projects of a similar kind have been undertaken or designed in other countries and, although a number of these may have left the Amsterdam equipment far behind as regards the attainable particle energy (as well as in size and cost), equipment such as the Amsterdam synchrocyclotron continues to fulfil an important function. In its own class this synchrocyclotron can be regarded as one of the best at present in operation, its special features being the very high beam current (and hence a high yield of radio-active substances) and its high degree of reliability in service.

Introduction

Three articles have already appeared in this Review on the subject of the Philips synchrocyclotron at the Institute for Nuclear Physics Research at Amsterdam [1]). In these articles descriptions were

---

*) Now professor at the Technical University, Delft.
**) Now attached to the South African Council for Scientific and Industrial Research at Pretoria.
[1]) F. A. Heyn, The synchrocyclotron at Amsterdam:
    I.   General description of the installation,
    II. The oscillator and the modulator,
    III. The electromagnet,
    Philips tech. Rev. **12**, 241-247, 247-256, and 349-364,1951 (hereinafter referred to as I, II and III).

given of the general scope and dimensions of this equipment, followed by details of the design of some of the essential components such as the oscillator, the modulator and the electromagnet. In the present article we propose to complete the series by saying something about the other main components and ancillary gear. Although numerous detail problems, were solved without fundamental knowledge — some, indeed, purely empirically — a description of them may well be useful, having regard to the fact that it is often just such details which

decide the success of a project. It may well be said, for example, that the high beam current in this synchrocyclotron (a good 20 µA) has to a large extent been achieved as a result of the empirical design of the ion source. The high degree of reliability, and in particular the

huge electromagnet, deuterium ions from the ion source describe circular paths in the Dees in such a manner that they are accelerated by the alternating voltage each time they pass the gap between the Dees, their orbits becoming larger and larger with each revolution. When some 5000 revolutions have been completed the deuterons have acquired an energy of 28 MeV and have then reached the region of
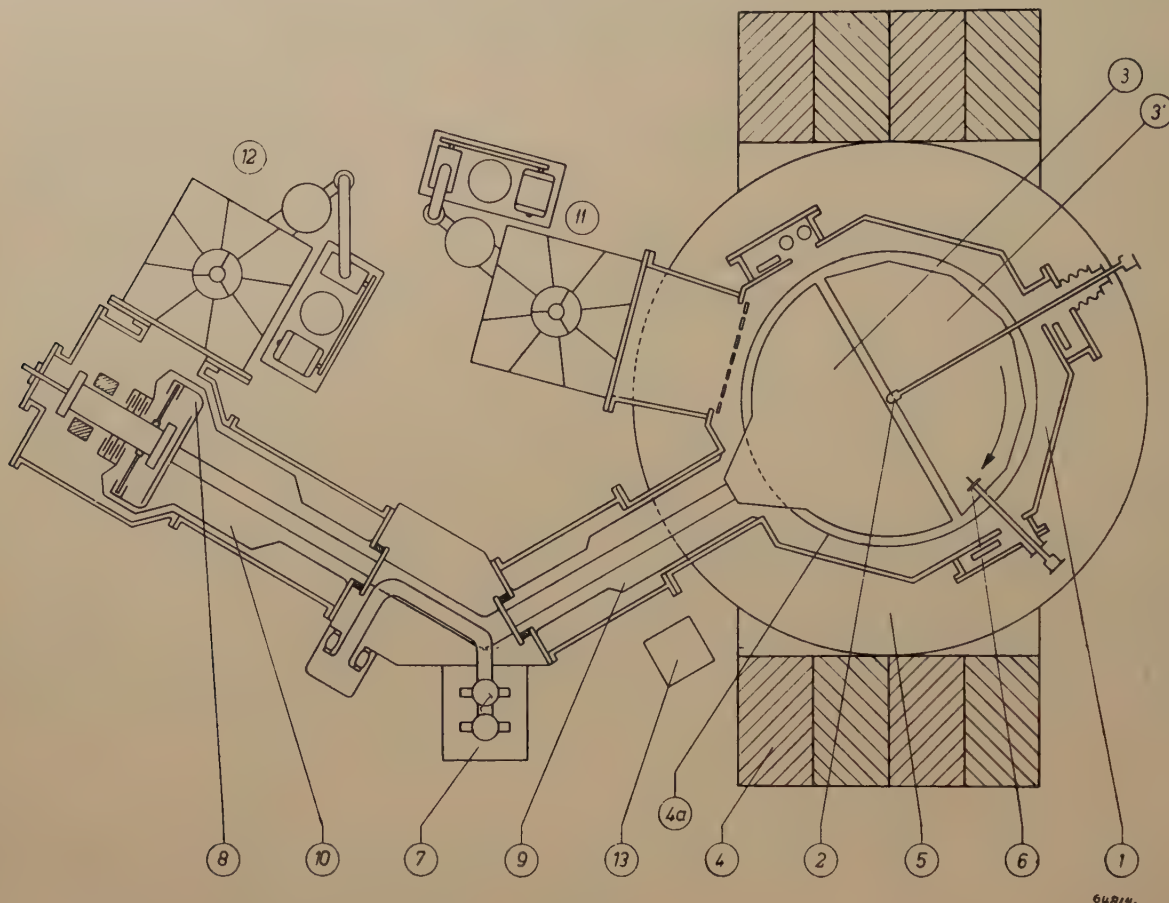
Fig. 1. Diagrammatic cross-section of the Philips synchrocyclotron at Amsterdam. *1* evacuated acceleration chamber; *2* ion source; *3* and *3'* Dees; *4* magnet (*4a* face of magnet pole); *5* energizing coils; *6* target; *7* valves and other components of the oscillator; *8* modulator; *9* and *10* coaxial transmission line; *11* and *12* vacuum pumps; *13* boron ionization chamber for monitoring the radiation emitted.

small amount of time wasted owing to interruptions during operation, may be ascribed to the unconventional design of the acceleration chamber and its associated components (which allow of rapid dismantling), the efficient construction of the vacuum system and the numerous safety devices provided to avoid errors in manipulation.

For the convenience of the reader a brief survey of the general design of the cyclotron is given, with reference to *fig. 1.* Inside the circular, evacuated acceleration chamber the two Dees are mounted, between which a high frequency voltage of about 10.7 Mc/s with a peak of roughly 14 kV is applied [2]). Under the influence of the magnetic field of the

the periphery of the acceleration chamber. Here they strike the target, upon which the material to be irradiated is placed. The oscillator generating the high frequency voltage, and the transmission line by means of which this is applied to the Dees are also visible in the diagram (fig. 1). The function of the modulator need not be discussed here; we refer the reader instead to I and II.

The acceleration chamber

The design of the synchrocyclotron was based on a maximum particle-orbit radius of about 80 cm, with a pole-piece radius of 90 cm. To suit these dimensions the acceleration chamber had to be roughly 2 metres in diameter. This chamber is evacuated to a very low pressure (about 10^{-4} mm Hg) to prevent loss of accelerated particles owing to collision with gas molecules.

---

[2]) At the present time the cyclotron is operated at 20 kV, so that the particles describe a smaller number of revolutions.

The top and bottom of the chamber have thus to withstand a pressure of something like 30 tons, and they can be supported only at the sides, since
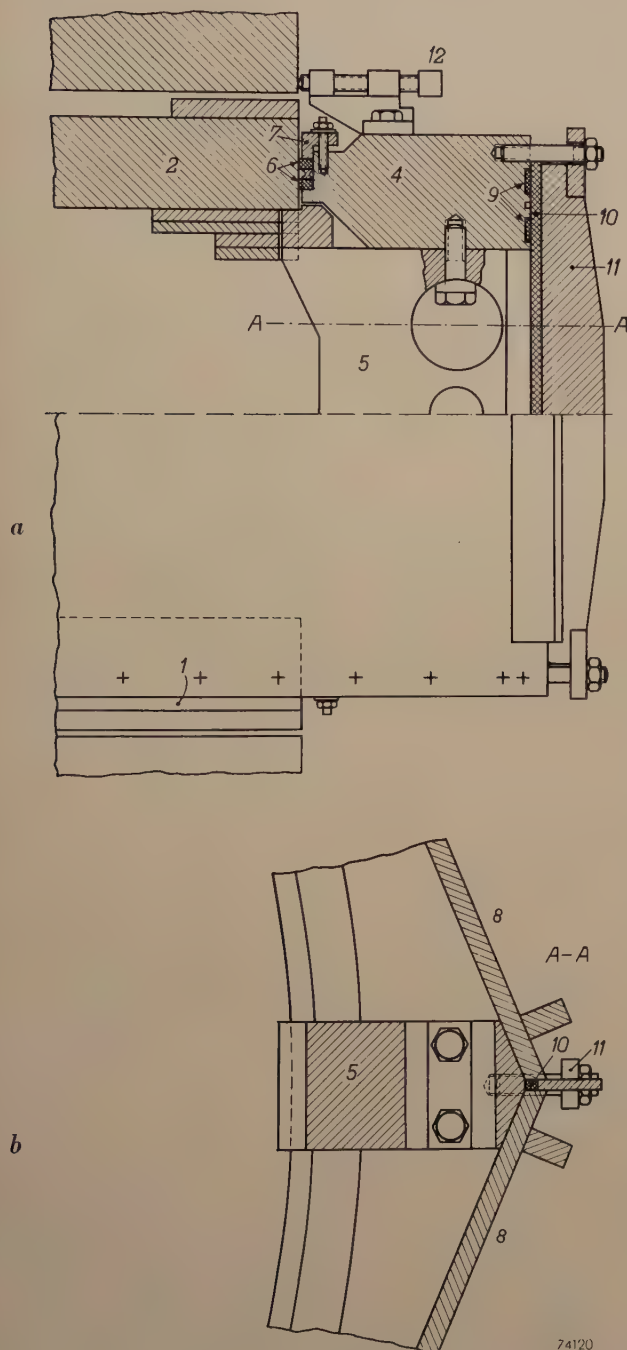

Fig. 2. One of the eight corners of the acceleration chamber: *a*) vertical cross-section, *b*) horizontal cross-section. *1* bottom plate; *2* top plate of the chamber; *4* upper brass ring; *5* brass pillar. The space between the rings and plates is sealed, vacuum-tight, by round-section rubber rings *6* pressed into a groove by packing clamps *7*. Two rubber strips *9* ensure a vacuum-tight joint between the brass rings and side plates *8*. The spaces between the side plate, which are 8 mm, are closed by means of 10 mm rubber cord *10*, held in place against the pillar by a heavy clamp *11*. This cord crosses the horizontal strips *9*, but proper matching of strip and cord, together with sufficient pressure, ensures an air-tight joint. *12* set-screw for centering the acceleration chamber between the magnet poles.

supports in the centre would obviously intercept the particles in their course. The best solution involves using the poles of the magnet themselves as top and bottom of the chamber. The large width of the magnet gap — which is responsible for the greater part of the 500 000 ampere turns required (see III) — is thus utilized to the greatest possible extent. This is important since the Dees should be given the greatest possible depth in order to minimize the loss of particles which oscillate, with considerable vertical amplitude in their initial revolutions and tend to collide with the top and bottom surfaces of the Dees.

To facilitate the "shimming" of the magnetic field (see III) and, more especially, to facilitate assembly of the acceleration chamber, in the final design 2-centimetre air-gaps were left in each pole, 7 cm from the face. Thus, the chamber in fact has separate top and bottom plates, each of these being 7 cm thick; these, however, are of the same material as the magnet itself. Being so thick, they hardly deflect at all under the atmospheric pressure. The supports at the sides are arranged symmetrically so that any buckling will also be symmetrical. The radial variation of the magnetic field, whose adjustment is very critical (see III), has been found to be undisturbed by the very slight buckling which occurs.

In order that the magnetic field shall not be affected in any way, it is essential also that everything between the top and bottom faces be made of non-magnetic material, including the vertical walls. Usually, the walls are made in one piece, of brass or non-magnetic steel and on which the top and bottom plates are laid, the assembly then being wheeled between the poles, or welded together when in position. Here we have tried out a new form of construction. The chamber is built up from elements of convenient size, so as to be easily demountable. The main components are: two cast brass rings with octagonal circumference, laid close around the top and bottom plates; eight brass pillars placed between the plates round the periphery and to which the rings are screwed; and eight rolled brass plates fitted to the sides of the rings. The chamber was built up from these elements directly between the poles. Airtight joints were obtained by means of rubber gaskets (see *figs.* 2 and 3). It should be pointed out here that, for the chamber to be demountable, crossings of rubber seals are unavoidable. Surprisingly enough, this works quite well, provided that each crossing involves one round and one flat rubber (not round-and-round or flat-and-flat). The total leakage into the acceleration chamber

built up in this way, as well as that of the connected spaces (oscillatory system for the Dee-voltage, pump lines etc.) is less than 10^{-5} litre (at normal atmospheric pressure) per second, that is, about 6 litres per week for a total volume of 2 cubic metres, which is quite acceptable.
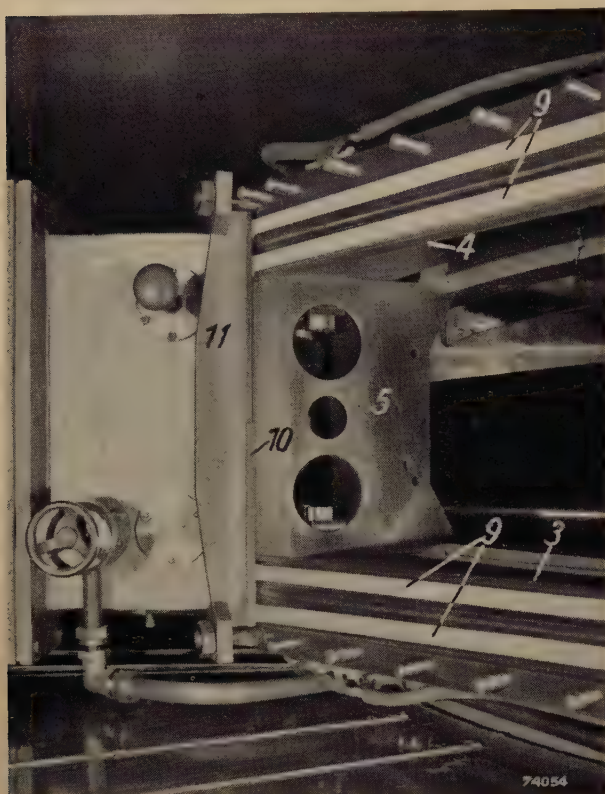

Fig. 3. A corner of the acceleration chamber with side plate removed, showing brass pillar 5 (see fig. 2) between the upper and lower brass rings (3 and 4), and the horizontal rubber strips (9), the rubber cord (10) (top half cut away to show detail), and the associated packing clamp (11).

The acceleration chamber is supported on the bottom pole by six brass spacers, 2 cm in thickness. When the magnetic field is applied it tends, by reason of the barrel-shaped pattern of the lines of force in the magnet gap (see III), to pull up the top plate against the forces of gravity and air-pressure. Since the top and bottom plates are able to move slightly on their seals, this displacement does not result in leakage; however, to limit the amount of movement, six brass blocks are included between the top plate and the upper pole, the thickness of these blocks being calculated to suit the pole spacing with the magnetic field in operation. In fact, owing to the mutual attraction of the poles, which causes the magnet-yoke to give slightly, the spacing in question is somewhat smaller than in the absence of the field. (This apparently insignificant constructional problem, which is solved quite simply by the

method of sealing employed, gave rise to much trouble in other cyclotrons.)

The inner faces of the top and bottom plates, as well as the shims at the edges (see III, fig. 4c) are clad with copper in order to reduce losses in the H.F. field of the Dees. Nevertheless, the heat developed as a result of losses is such that water-cooling must be employed.

The Dees

Of the two Dees in the acceleration chamber the one is earthed whilst the other carries the 14 kV H.F. voltage with respect to earth. The latter is suspended on a stem (9, fig. 1) which functions also as a transmission line; the end of this stem is clamped between two rings with "Kersima" insulators (see II) and each of these rings is held in place by four pins (fig. 4), by means of which the Dee can be adjusted so as to lie parallel to the earthed Dee. The gap between the Dees is 5 cm.

In view of the limited (though fairly high) compression resistance of the insulators and to avoid too much sagging, the Dee and its stem are fabricated from a light framework of brass, jacketed with copper. The top and bottom halves of the jacket are water-cooled; the cooling system is illustrated in fig. 4.

The height of the mouth of the Dee was made as large as possible, viz. 20 cm, in order to hold as many particles from the ion source as possible and, as already mentioned, to minimize the loss of particles owing to collisions with the top and bottom surfaces. It was not possible to use a larger mouth height in the Dees in conjunction with the given magnet gap, in view of the risk of flashover to the top and bottom plates of the chamber. Furthermore, the capacitance of the Dee should not be too high (see II). For the same reason the Dee decreases in height towards the periphery of the acceleration chamber, where the oscillation amplitude of the particles is smaller; at the point where the radius of the path is the greatest, the height of the Dee is 10 cm. The earthed Dee, which consists of plates attached to the top and bottom of the chamber, presents to the particles roughly the same amount of space as the other Dee.

The housing containing the stem of the Dee is mounted on a carriage and can be moved on rails, enabling this Dee to be easily removed from and re-introduced into the acceleration chamber; for this purpose two of the columns and two side plates must be removed.

The ion source

It has already been pointed out that a copious source of ions is necessary to ensure high beam intensity. This is all the more important since only a fraction of the ions produced are accelerated; acceleration of the particles can commence only at the beginning of each modulation cycle (see II) and, further, only those particles are accelerated which, in a certain phase of the Dee voltage, occur at a certain point, such that the phase stabilization operates in their favour.

Quite a number of designs were tried out for the ion source and the following was ultimately found to give very satisfactory results. The gas to be

with respect to the earthed walls, this voltage being applied through a current limiting resistor. Owing to the relatively high pressure in the chamber, a gas discharge occurs, as a result of which the tungsten becomes incandescent and emits electrons (an operating voltage of 210 V gives rise to a total current of 150 mA). On account of the presence of the intense magnetic field the electrons are able to move only in narrow helices around the magnetic
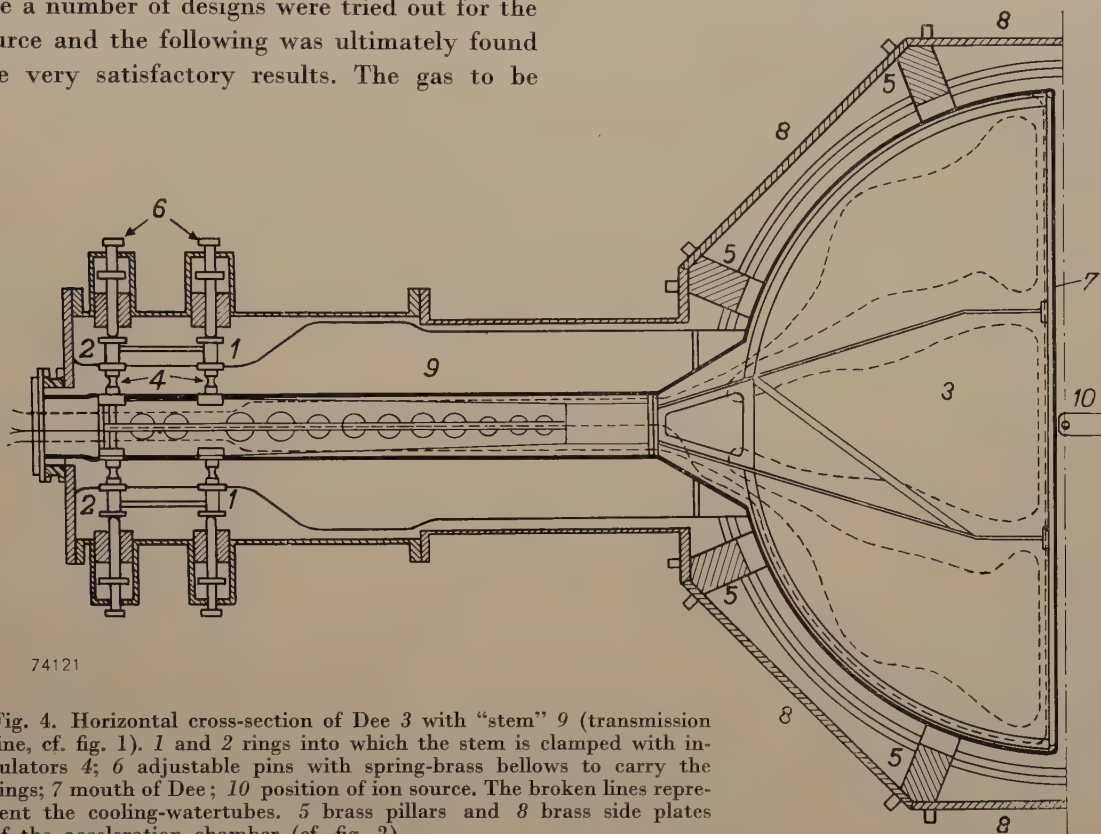

Fig. 4. Horizontal cross-section of Dee 3 with "stem" 9 (transmission line, cf. fig. 1). 1 and 2 rings into which the stem is clamped with insulators 4; 6 adjustable pins with spring-brass bellows to carry the rings; 7 mouth of Dee; 10 position of ion source. The broken lines represent the cooling-watertubes. 5 brass pillars and 8 brass side plates of the acceleration chamber (cf. fig. 2).

ionized, usually heavy hydrogen, is supplied to an earthed copper chamber located just above the gap between the Dees. This chamber is fitted with a nozzle, directed downwards in the direction of the magnetic lines of force (fig. 5) and through which gas will enter the accelerating chamber. The orifice of the nozzle is sufficiently long (60 mm) and narrow (5 mm diam.) to ensure considerable difference in pressure between the two extremities; with a flow of gas of 0.085 cc/sec (about 0.3 litre per hour referred to 76 cm Hg), the pressure inside the chamber of the ion source is 0.1 mm Hg, whereas the pressure just downstream of the nozzle is a good 10^{-4} mm Hg. Inside the chamber there is a horizontal tungsten pin, 4 mm thick, mounted in insulating material and carrying a voltage of —450 V
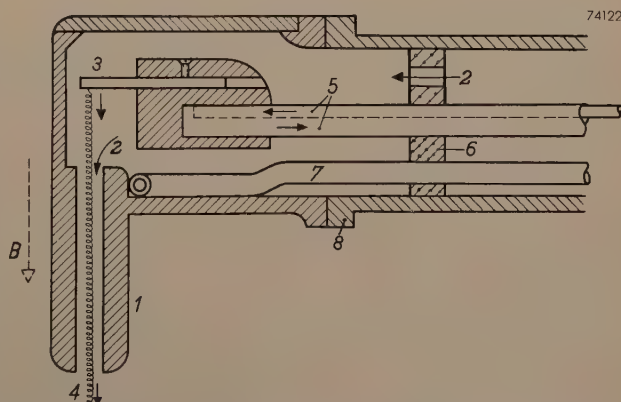

Fig. 5. The ion source. 1 narrow-bore nozzle, parallel to magnetic field B; 2 gas inlet; 3 tungsten pin; 4 electron stream; 5 cooling tubes (also current conductor for the tungsten pin); 6 insulator; 7 cooling tube for walls of chamber; 8 flange to which the ion chamber is screwed.

lines of force which are parallel to the nozzle. Hence a highly concentrated electron beam issues from the nozzle and passes through the acceleration chamber, arriving finally on a water-cooled plate

cathode, and so on. The electrons, thus passing repeatedly to and fro through the nozzle, produce sufficient ions there to maintain the tungsten cathode at a high temperature by the ion bombardment,
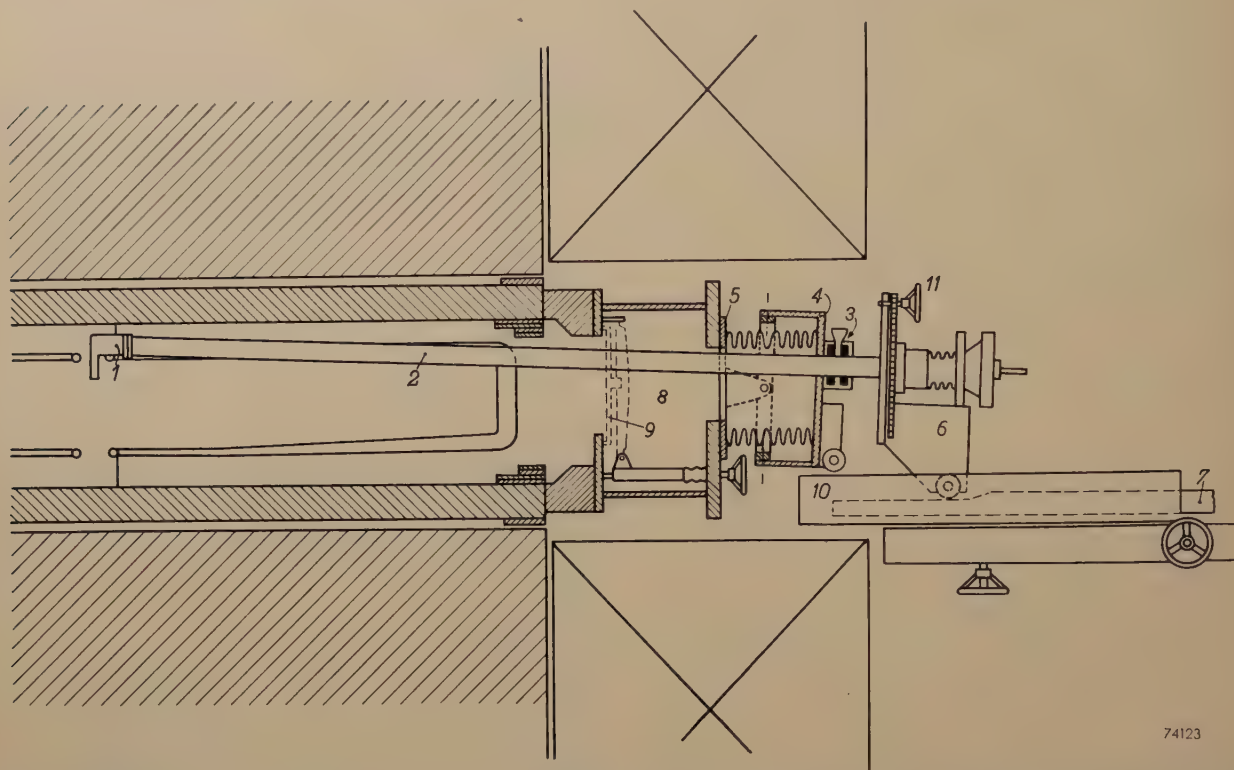

74123

Fig. 6. Holder and controls of the ion source. *1* ion chamber with nozzle; *2* tube carrying ion chamber, containing insulated tube for the cathode and cooling tube for the chamber walls. The end of the long tube is supported by a bearing on carriage *6*. Plate *4* is another bearing in which the tube slides through a vacuum-tight gland *3* (consisting of two rubber seals with vacuum oil between them). The ion source can be inserted more or less deeply into the acceleration chamber by means of a handwheel *11*. Further, plate *4* can be tilted in two directions with respect to the flange *5* to which it is attached by spring-brass vacuum-tight bellows, enabling the ion source to be moved up and down or sideways in the Dee gap. That position of the ion source which yields the highest beam current can thus be found while the cyclotron is operating. In order to withdraw the ion source from the acceleration chamber, for example to renew the tungsten pin, the carriage *6* is pulled back along the rails *7*. When the ion source reaches the vacuum lock *8*, the cover *9* is closed (see fig. 8) and the flange *5* can then be loosened; the flange, with plate *4* and the whole ion source assembly, is then retracted on the rails *10* which are first raised so that the wheels on plate *4* come to rest on them.

at the bottom of the chamber. The electrons spiralling downwards have to cover a considerable distance, and they thus produce in the acceleration chamber a very large quantity of ions, even though the gas pressure there is low.

It is not yet possible to explain in every detail the action of this ion source (which might better be referred to as an electron source). It is worthy of note that the gas discharge in the source is extinguished immediately the H.F. Dee voltage is cut off; furthermore, in the absence of this H.F. voltage, it is not possible to start up the source at the above-mentioned ignition potential of 450 V. Probably, the explanation is that, in the negative phase of the Dee voltage, the electrons are reflected from the Dee field, thereby resume a helical path upwards through the nozzle, are again reflected by the
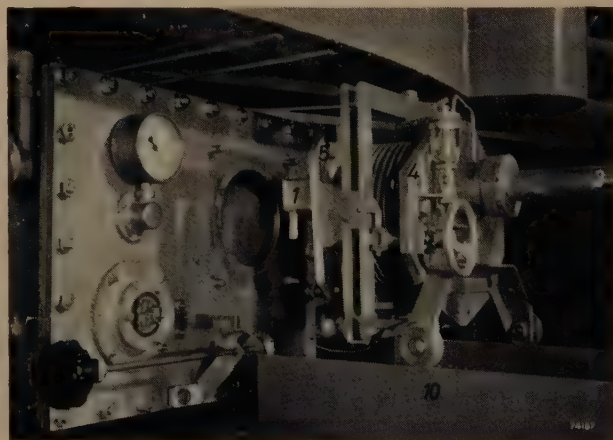

Fig. 7. The ion source fully retracted. In the photograph will be seen: *1* the ion source chamber; *2* tube, *3* gland; *4* plate and *5* flange on the bellows; *10* rails on which the wheels on plate *4* run.
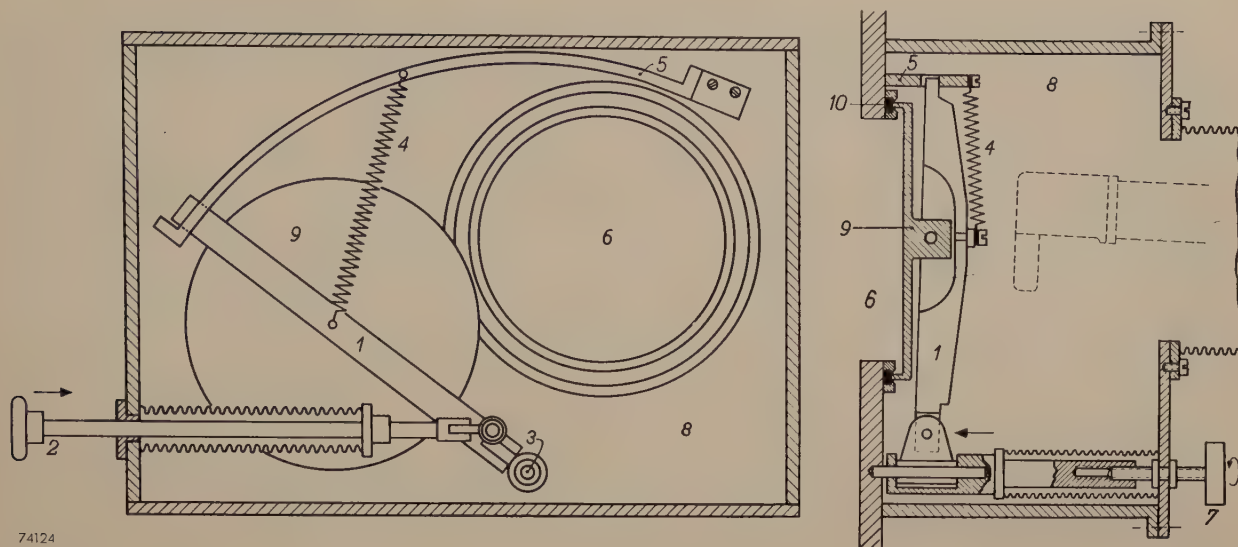
74124

Fig. 8. The vacuum lock for the ion source. Cover 9 (cf. fig. 6) is mounted on an arm 1 which, when the pin 2 (with bellows) is pushed in, swings on a pivot 3. This demands little effort as the movement is assisted by a spring 4. When the arm is rotated, the extremity slides on a track 5 until it reaches a stop, in which position the cover is exactly in front of aperture 6 in the acceleration chamber (through which the ion source has already been drawn; this is indicated by the broken lines on the right-hand side of the cross-section). When the handwheel 7 is turned, the lower end of the arm 1 is pushed inwards by a screw spring-brass bellows, so that the cover 9 is pressed firmly against a packing ring 10. Air can then be admitted to the trap.

i.e. an independent discharge occurs. In order to ensure the emission of sufficient electrons to sustain this process (and to provide the necessary heavy ionization within the acceleration chamber) in spite of the large space-charge in the nozzle, the nozzle must not be too narrow. Experience has shown, in fact, that the discharge cannot be established with, for example, a 4 mm nozzle.

The tungsten pin is held in a water-cooled copper block (fig. 5). The cooling tube serves simultaneously as support and as conductor for the feed to the pin. To prevent the extremity of the pin from being cooled too much, this pin must be of a certain minimum length. The walls of the ion source are likewise water-cooled.

Outside the acceleration chamber the tube carrying the whole ion source assembly is carried on a plate which is adjustable in two directions, in such a way that the most satisfactory position for the source can be found when the cyclotron is in operation. The tungsten pin has to be renewed every other day, since the yield of ions drops owing to melting and evaporation of the tungsten; to facilitate replacement, a vacuum lock is incorporated through which the source can be withdrawn without admitting air to the acceleration chamber. The mechanical design may be seen from figs 6, 7 and 8, in whose subscripts further details are given.

Fig. 9. Valve assembly for continuous feeding of the ion source with gas (heavy hydrogen or helium) at constant pressure. 1 storage bottle; 2 mechanism for giving signal in control room as soon as pressure in the storage bottle drops below 10 cm Hg, i.e. warning that bottle must be renewed; 3 buffer volume in which pressure is kept practically constant; when pressure drops, the switch 4, operating through spring-brass bellows, actuates an electromagnet 6 which opens the inlet valve 7 a little more; 8 duct offering high resistance to flow of gas, to damp out fluctuations; 9 needle valve to regulate gas supply to the ion source (operated from control room by means of a servomotor); 10 gas line to ion source; cocks 11, 12, 13 and 14 are used for withdrawing air that enters when the gas storage bottle, or the tungsten pin in the ion source is renewed; 15 and 16 are connections for pressure gauges; 17 stop cock.
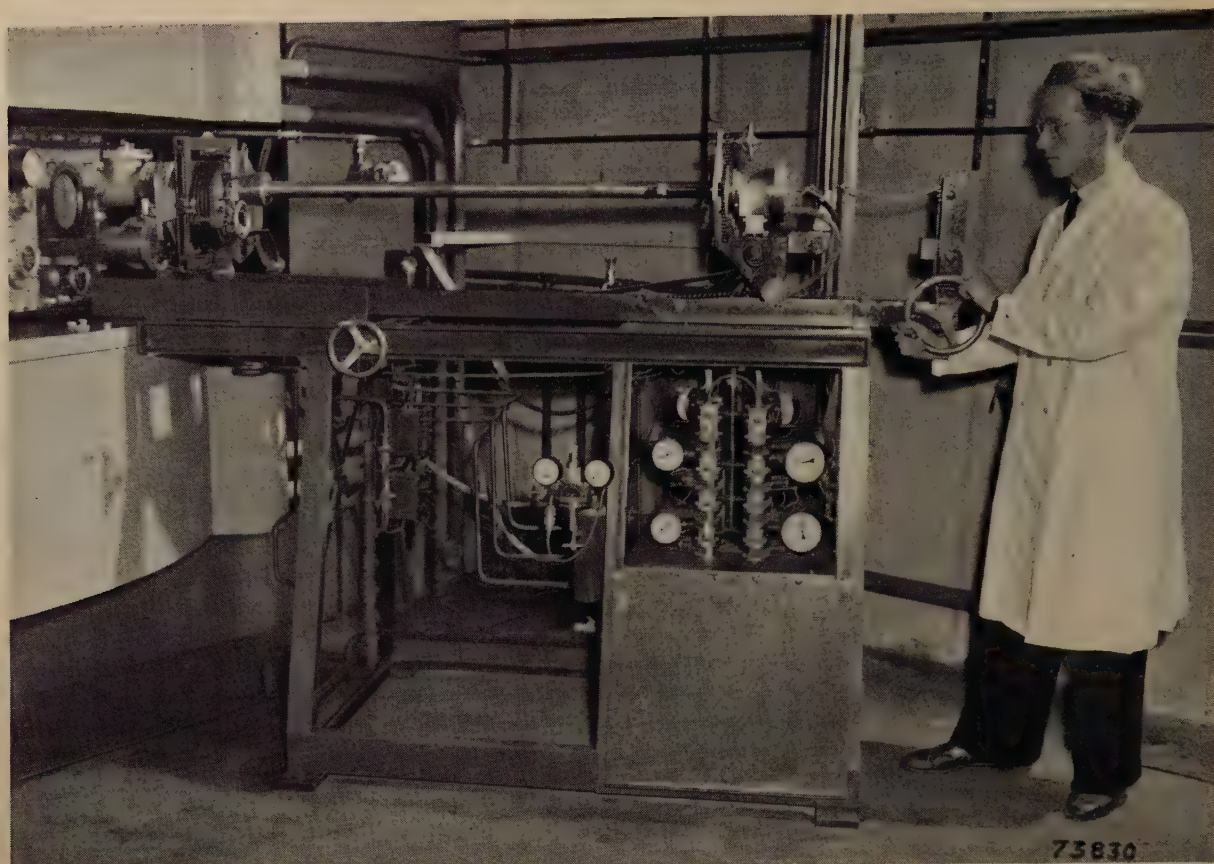
74125
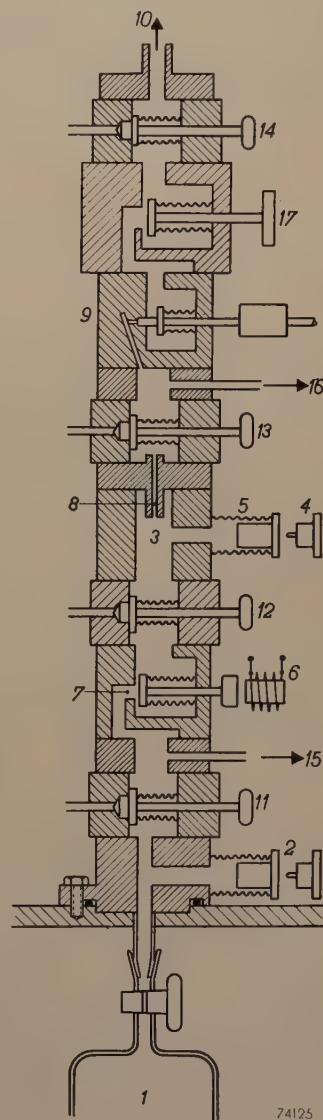
Fig. 10. The complete apparatus associated with the ion source. The source is shown withdrawn from the chamber. Below, in the framework supporting the rails, is the gas supply apparatus, which is duplicated for the acceleration of helium or deuterium ions as described. The two glass storage bottles are housed in the compartment below. The consumption of gas is 0.3 litre per hour (referred to 76 cm Hg).

The heavy hydrogen, which has to be continuously supplied to the ion source, is obtained from heavy water by electrolysis and is stored in glass bottles, the pressure in the chamber of the ion source being regulated by means of a needle valve. To avoid the necessity of constant readjustment of the valve while the bottle is emptying, a buffer volume is included between the valve and the bottle, in which the pressure is automatically kept constant. The buffer volume contains a spring-brass bellows which contracts when the pressure drops, and trips a switch; this, with the aid of an electromagnetic control, opens the valve to the buffer volume more; the pressure then rises to the normal level and the expanding bellows once more reduces the gas supply. This "discontinuous" control of the pressure does certainly produce in the buffer volume small variations about a pre-set, average, value, but owing to the high resistance encountered in a narrow duct between the buffer volume and the valve, these variations are not passed on to the ion source to any noticeable extent.

Fig. 9 is a cross-section of the gas supply system, showing sundry other components; fig. 10 is a photograph of the complete equipment associated with the ion source.

The target

The beam of accelerated particles, spiralling outwards, comes more and more into focus and finally strikes the target, on which the substance
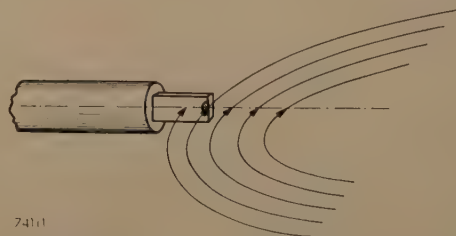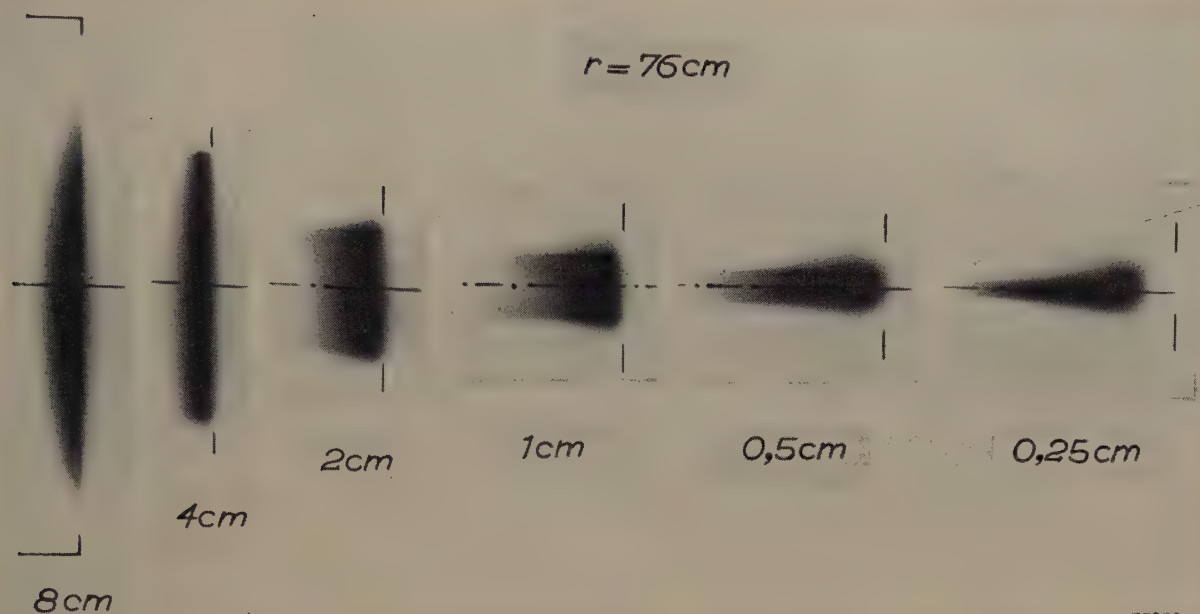

Fig. 11. Location of the target with respect to the beam of accelerated particles. These strike the target mainly within the area shown hatched.

to be bombarded has been placed; the manner in which this takes place is illustrated diagrammatically in fig. 11.

At the target the great heat generated constitutes

Fig. 12. Distribution of intensity of the beam on the target, with targets of different vertical dimension, at a radius r of 76 cm in the acceleration chamber. The lines indicate the position of the edge of the targets. These illustrations are contact prints on a photographic film, of a set of copper plates, each of which was placed in the beam for a few moments (autoradiograms). With the plates of small height, the prints show considerable over-exposure; in the case of the 0.25 cm plate, which was not easy to cool, the front end has melted off.
For more quantitative details of the beam distribution, the activity is measured at a number of points on the activated plates with a Geiger counter.

quite a problem; with a particle energy of 28 MeV and a beam current of 20 μA, the beam dissipates 560 W at the target, a large part of the power being concentrated within the hatched area shown in fig. 11. This repeatedly gave rise to evaporation and melting of the substance irradiated and efficient dispersal of the heat became an all-important problem.

If the beam were confined to the median plane of the acceleration chamber (and if the component sections of the path of the particles were truly circular), all the particles would be intercepted by the edge of the target where this is intersected by the median plane. Actually, however, the vertical spread of the beam is considerable, in consequence of the vertical oscillation of the particles. Many particles therefore shoot past the target, above or below it, perform one or more extra revolutions, thus acquiring a larger path radius, and finally strike the target at points away from the tip. (A similar effect is produced because, owing to radial oscillation, each particle does not describe an expanding circle, but an expanding and precessing ellipse). If a longer target (in the vertical direction) is used, most of the particles will be intercepted at the edge, giving a high, narrow impact area; if the target is made any smaller in the vertical direction, more particles will be able to continue on their spiral path and the impact area will be low and wide, as will be seen from *fig. 12*. For the production of radio-active substances a uniform field is most favourable and a target of average height is therefore used.

It is also interesting to note the modification in the form

of the beam when the radius is varied. This modification is illustrated in *fig. 13*, from which it will be seen that the beam is not invariably symmetrically disposed with respect to the median plane; also that the height decreases when the radius is increased. (With a sufficiently small radius, i.e. much lower particle energy, the beam covers the whole height of the Dees [3]), the beam current as measured there being some hundreds of microamps.) Particles can be detected beyond even the normal working radius of 78 cm.

The heat developed at the target is carried away by a water-cooling system. Often the substances to be bombarded are made into high melting-point compounds (glasses) which are applied in the form of a thin layer to a copper water pipe. Where this is not possible, a block of metal is soldered to a water pipe and holes of, say, 1 mm diam. are drilled in the block, into which the substance in question is introduced. Metals to be bombarded are clamped between two water-cooled plates. A number of targets of different kinds is depicted in *fig. 14*; the long tubes for the water-cooling serve at the same time as holders when the radio-active or "hot" substances are removed or further handled. The target is changed in much the same way as the ion

[3]) It has been noticed that the Dees themselves become radioactive at certain points, which indicates that they are struck in these points by parts of the beam.
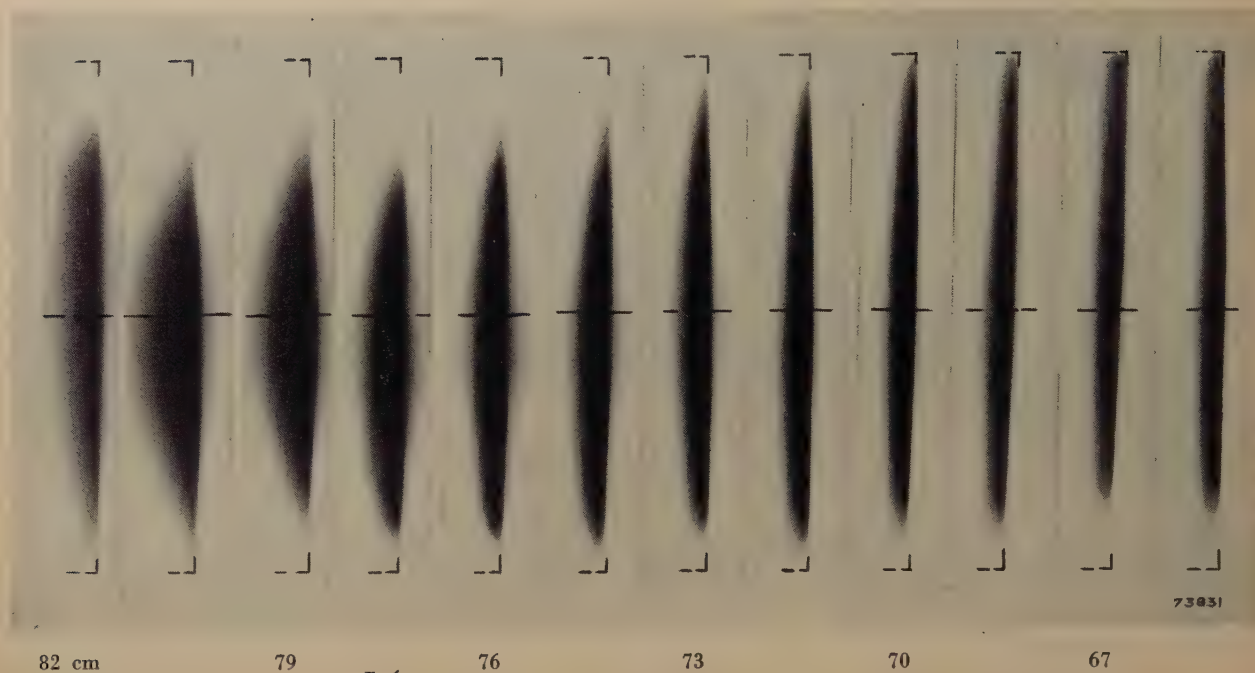
82 cm   79 $r \leftarrow$ 76   73   70   67

Fig. 13. Exposures of the beam as in fig. 12, obtained with one target 8 cm in height placed at different orbit radii r.

source, with the aid of a vacuum lock. This is very similar in design, except that all the controls are now at the rear, since personnel always have to keep at a safe distance from the "hot" material (*fig. 15*).

The depth of penetration of the target into the acceleration chamber can be increased or decreased so that it is struck by particles of lower or higher energy, and the actual position is indicated by a scale, calibrated in MeV. The energy can also be checked by measuring the range of the particles: Several thin targets are then placed one behind the other; the higher the particle energy and therefore the greater the number of particles passing through the first targets in the series, the greater

Fig. 14. Different types of target. These are handled by the long tubes which serve for the water-cooling.
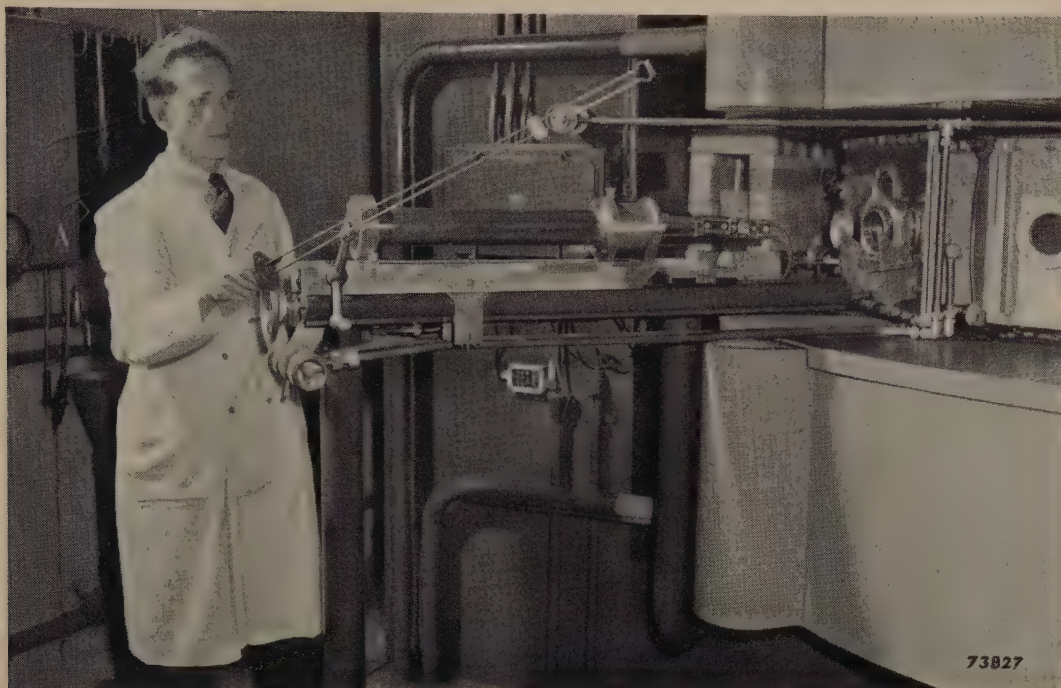
Fig. 15. The target is changed through a vacuum lock similar to that provided for the ion source; all manipulations are such that the operator remains at a safe distance from the "hot" target.

will be the effect produced at the later targets.

For regular production of radio-active substances it is important that the beam current be monitored continuously. This is effected in the equipment under discussion by measuring the temperature rise of the cooling-water at the target (*fig. 16*). The flow of water is kept constant by letting it run from a constant head tank. A multiple thermojunction is incorporated in the outgoing and return pipes and the thermo-current, which is a direct measure of the heat generated at the target, may be registered continuously by an instrument in the control room of the installation. In this way a direct record may be obtained of the performance of the cyclotron (the

Fig. 16. The target *1* is cooled with water flowing from a reservoir *2* in which a constant head is maintained (*3* is an overflow). The rise in the temperature of the cooling water is measured continuously by the multiple thermojunction *4*, this rise being a measure of the beam current in the cyclotron. Calibration is possible by means of a constantan coil *5* which dissipates a known amount of power.

number of μA-hours) during a given period. Since the flow-resistance of the whole cooling system is likely to vary, e.g. owing to differences in the form of the target, a calibration of the current measurement is necessary for each target. To carry out this measurement, a spiral of constantan wire is mounted in the cooling-water pipe, and a stabilized voltage can be applied so as to dissipate a known amount of power in the water.

In order to determine the performance of the cyclotron itself accurately, the effect of thermal radiation at the target must be eliminated. For this purpose, a thick copper target is used whose temperature hardly rises at all since its thermal conductivity is high.
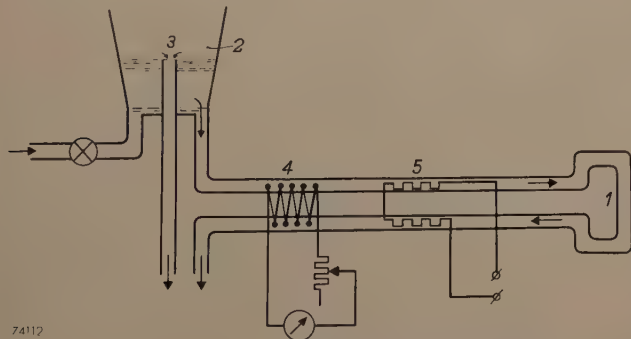
The vacuum pumps

We have seen above that, to ensure a high beam current, a relatively high gas pressure is required in the ion source, together with a low pressure (about 10^{-4} mm Hg) in the acceleration chamber; in addition, the duct between the ion source and the acceleration chamber must not be too narrow. To satisfy these conflicting requirements the acceleration chamber has to be connected to a very high speed vacuum pump. At the same time the pump has to cope with the air-leaks which were mentioned above (and which could not be estimated accurately in advance) and it has to pump away any gases that may be liberated from the large metallic sur-
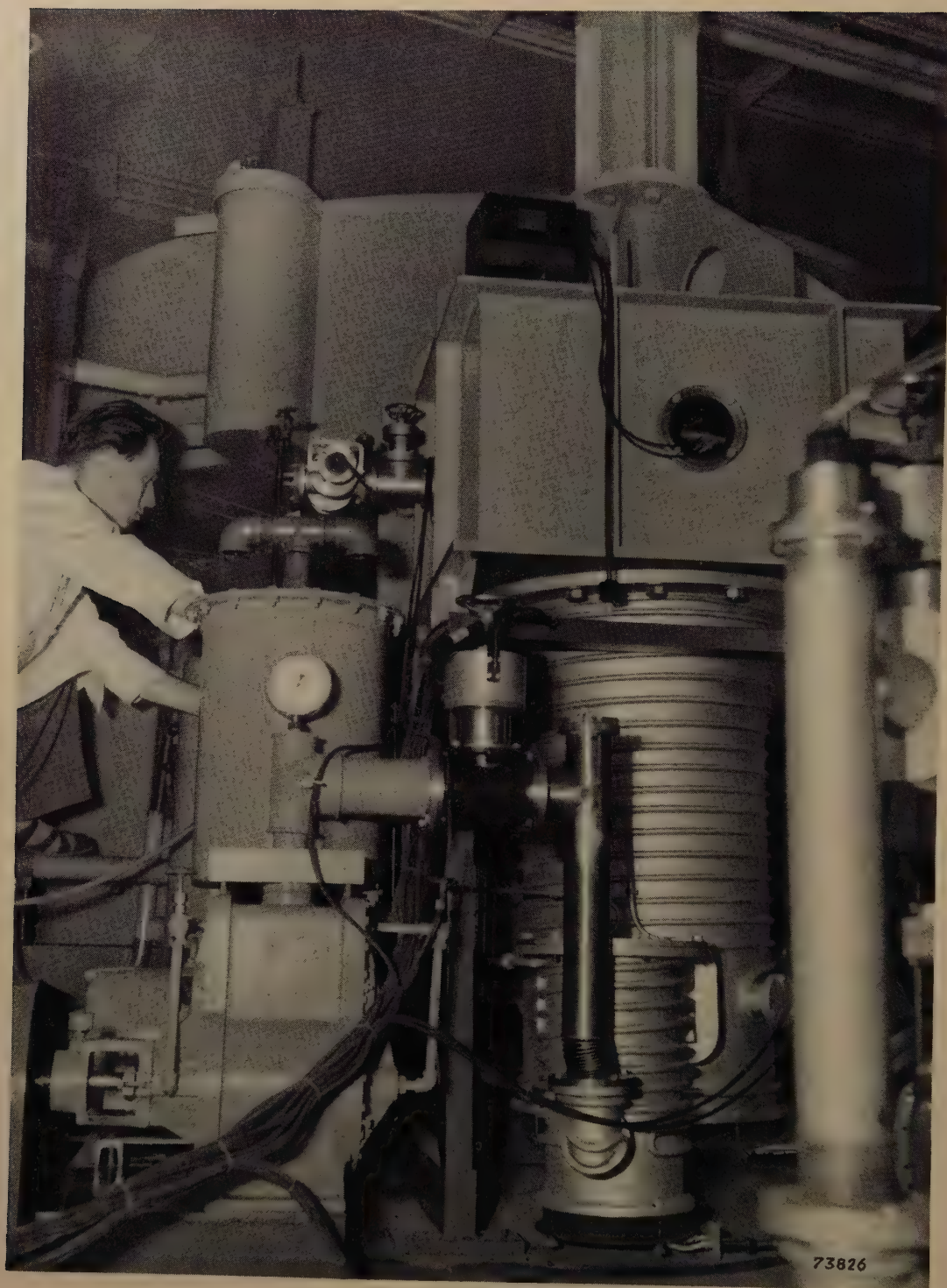
Fig. 17. One of the high-vacuum pumps of the cyclotron. On the right, below, will be seen the large cylinder comprising the 3-stage vapour diffusion pump and, in front of it, the booster pump, both with cooling-water tubes round the outside. On the left is the rotary backing pump. The valve and vapour trap are seen above the large cylinder and, behind these, the upper energizing coil of the magnet.

faces present. The general indication for the design of the pump was, therefore, that the pumping speed must be "as high as possible". Owing to unavoidable flow resistance, however, the pressure in the acceleration chamber, beyond a certain pumping speed is further reduced only very slightly (see below). Carefully prepared estimates indicated that a pumping speed S_0 of 3000 litres per sec as measured at the pump should be aimed at. For comparative purposes it may be noted that normal good quality commercial mercury-vapour diffusion pumps have a pumping speed of say $S_0 = 50$ l/sec,

the speed of the largest vacuum pumps at present obtainable being 15 000 l/sec.

The pumping system designed by us, of which a photograph appears in *fig. 17*, comprises the usual backing pump and a 4-stage diffusion pump, viz. a booster and a 3-stage main pump. *Fig. 18* depicts the diffusion and booster stages diagrammatically.
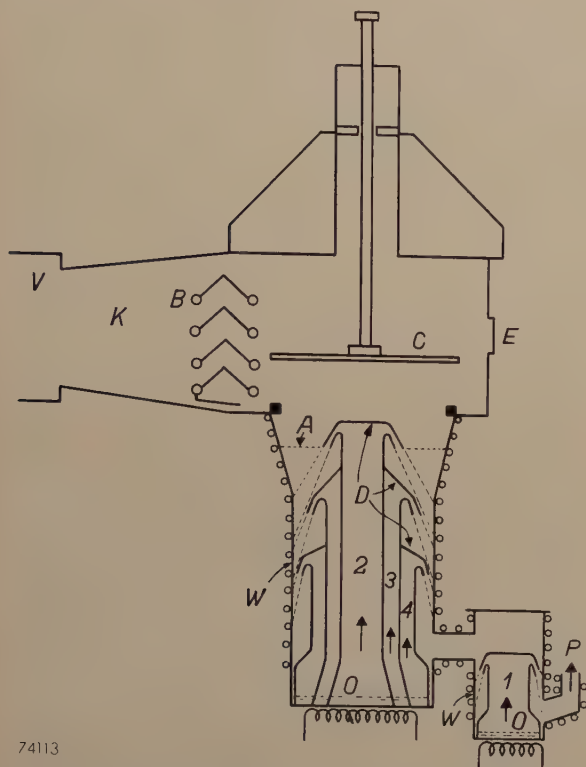

Fig. 18. Diagrammatic cross-section of the oil-vapour vacuum pump. *O* boiling oil; *1, 2, 3* and *4* chimneys of the four stages; *D* deflectors; *W* water-cooled casing. *P* backing line; *A* inlet aperture of the pump; *K* pump duct; *B* vapour trap; *C* valve. The plates of the vapour trap are cooled by a "Freon" refrigerator; they are tinned to promote reflection of the heat rays falling on them, and the whole assembly of plates is mounted on two thermal insulators. *E* inspection window, also to be seen in fig. 17. *V* acceleration chamber of the cyclotron.

At the bottom of the pumps there is a quantity of oil (Silicone Fluid DC 703) which is raised to boiling point by a heater. The vapour from the boiling oil rises through four "chimneys" in which the pressure is some tenths of a millimetre of mercury and deflectors direct the vapour through small annular outlet slots. From the chimney of each stage, therefore, a stream of vapour passes obliquely downwards. The walls against which the vapour jets strike are well cooled with water and the vapour is thus practically all condensed; accordingly, nearly all the vapour molecules move downwards at a high velocity (average value v_d). Gas molecules entering the pump by way of the inlet (A) and coming into contact with the vapour jets are drawn with the vapour; below the jets the gas is

thus "compressed", the jets forming a barrier between a zone of low pressure above and one of higher pressure below.

In fig. 18 three other elements will be seen between the acceleration chamber and the pump proper, viz. a pump duct K, a vapour trap B and a valve C. The vapour trap serves in the first place to prevent oil vapour and the products of decomposition of the oil from entering the acceleration chamber; it consists of a number of metal plates in the form of inverted Vees, thermally insulated from the body and so arranged that no gas or vapour molecules can pass them without striking them at least once. The expansion tube of a "Freon" refrigerator is soldered to the plates and the temperature of these plates at the coldest points is —30 °C; any oil vapour is thus almost wholly condensed on the plates (the oil vapour pressure at the temperature in question is $< 10^{-6}$ mm Hg). Furthermore, the trap prevents an excess of water and other condensable vapour (grease and other impurities) from passing from the acceleration chamber to the pump and at the same time it assists in removing such vapours from the chamber. (Residual water and other vapours are gradually eliminated from the acceleration chamber at the commencement of each working period by means of a number of liquid air traps, connected to it.) The valve, which rests on a rubber seating, is used to close down the pump for the night, in order to prevent vapours from the pump or air from the low-vacuum volume from finding their way into the acceleration chamber [4]); this valve must not be opened until the pump is in full operation. On the other hand, closing of the valve also protects the pump in the event of an accident (breakage in any of the equipment connected to the chamber) that might allow large quantities of air to enter, for this has a deleterious effect on the fluid. The presence of the third component mentioned above, the pump duct (80 cm × 50 cm cross-section), is purely a disadvantage, but is unavoidable, since the pump cannot be placed any closer to the acceleration chamber in view of the size of the energizing coils of the magnet.

The three components mentioned, together set up a certain flow resistance (referred to in our dis-

---

[4]) Small quantities of oil vaporize from the vapour trap during the night and enter the acceleration chamber, but these do no harm. This does, however, illustrate the reason why an oil vapour pump and not a mercury vapour pump should be used; mercury vapour penetrating into the acceleration chamber would do incalculable damage by attacking the brass components, soldered seams etc. Another reason is that, in order to secure the required low pressure using mercury, it would be necessary to employ a vapour trap of much more complicated design, which would in turn increase the flow resistance.

cussion of the necessary pumping speed), so that
a difference in pressure occurs between the pump
inlet and the outlet of the acceleration chamber.
Let us denote the (constant) pressures at these
points by p_0 and p respectively, and the volumes
of gas flowing per second (the local pumping speeds)
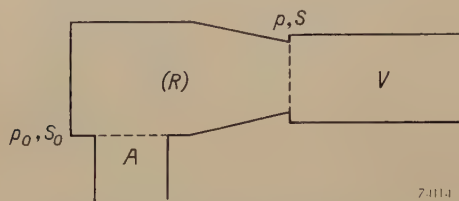S_0 and S respectively (fig. 19). Then, since the mass

Fig. 19. In order to secure a pumping speed S at the accelera-
tion chamber V against a pressure p, a greater pumping speed
S_0 with lower p_0 is required at the pump inlet A, in view
of the flow resistance (R) set up by intermediate elements in
the pumping duct.

of the gas is the same at both points, $S_0 p_0 = Sp$;
further, $p - p_0 = RpS$, where R is the flow resis-
tance, as defined by this equation. From the two
expressions t at once follows that:

$$\frac{1}{S} = \frac{1}{S_0} + R \ldots \ldots \ldots \quad (1)$$

It will be seen that S, the pumping speed at the
chamber, can never be more than $1/R$, even if the
speed S_0 of the pump itself were infinitely high. In
the pump under discussion, $S_0 = 3500$ l/sec for
air at a pressure $p_0 = 0.8 \times 10^{-4}$ mm Hg. After
completion of the whole installation, a pumping
speed of $S = 2200$ l/sec was measured at the
acceleration chamber; hence the resistance is $R \approx$
1.5×10^{-7} sec/cm³, which is lower than was anti-
cipated. (In view of the dimensions of the duct etc.,
we had estimated that R would be about 5×10^{-7}
sec/cm³). Had we designed the pump for $S_0 = 7000$
l/sec, which would have been much more costly,
the effective pumping speed would not have been
increased to more than 3000 l/sec.

We cannot here enter too deeply into the working
of the pump, but will mention only one or two
points. The design is dependent to a considerable
extent on the fact that it is mainly hydrogen, not
air, that has to be pumped from the acceleration
chamber. The vapour diffusion type of pump de-
pends for its action on the incoming gases being
entrained with the stream of vapour. Now,
hydrogen is entrained at a higher rate and for this
reason the pumping speed is appreciably higher
than with air (theoretically by a factor of 3.78). At
the same time, however, the gases are diffusing
against the vapour stream at a certain speed, de-

pendent on the local pressure, thus obviously re-
ducing the pumping speed, and this "back-diffusion"
is more pronounced in the case of hydrogen than
with air. To limit the effect of such "back-diffusion"
as much as possible it was necessary to arrange for
a very low backing pressure, a long stream of vapour
and high vapour velocity v_d. In this regard careful
dimensioning of the outlet slots and the choice of
the lightest grade of oil were important; v_d is
also increased according as the vapour pressure
of the oil is raised (by greater heating of the
boiler), but there is not much to be gained in this
direction, as this results in too much dispersal of the
vapour stream. The length of the stream is limited
for the same reason, and the desired large "pumping
distance" must therefore be achieved by means of
stages in cascade.

On account of all these factors, the speed of our
pump is roughly 4500 l/sec for hydrogen, this being
about 1000 l/sec more than for air. Moreover, the
flow resistance in the exhaust duct etc. (R in equa-
tion 1) is lower for hydrogen than for air, and this
represents a further improvement in the pumping
speed at the acceleration chamber.

The synchrocyclotron also includes another
vacuum pump for evacuating the modulator drum
(see I and II), but this pump does not have to meet
such stringent requirements; a speed of the order
of 500 l/sec is sufficient. None the less it was con-
sidered simpler and cheaper to make a pump iden-
tical with the one just described.

The pressure on the outer wall of the acceleration
chamber (and also at other points) is monitored
continuously by a Philips vacuum gauge (Penning
type [5])), an instrument that is well able to with-
stand sudden increases in pressure arising from
possible faults occurring in the cyclotron. The action
of this gauge depends on a gaseous glow discharge
in a magnetic field; in the region in question the
field of the cyclotron magnet — which is already
available — is used. By making the electrodes of
iron 3 mm thick it was found possible to reduce
the flux density inside the discharge space to the
required value of 0.04 Wb/m². Some of the pressure
gauges used are fitted as warning devices; the
electric discharge current flowing in the vacuum
gauge, which is a measure of the pressure, is taken
through an adjustable resistor and, at a given
value, the voltage across this resistor ignites a
mercury vapour tube, which in turn operates a
warning signal by means of a relay. One such gauge
incorporates an interlocking circuit that prevents

[5]) See Philips tech. Rev. **2**, 201-208, 1937; **11**, 116-122, 1949.

the ion source from being switched in on the event of the pressure being too high, thus protecting the tungsten pin in the source from premature deterioration.

This brings us to the various safety devices, regarding which we shall say something in the following paragraph.

Controls and safety devices

To give an impression of the synchrocyclotron as a whole, after digressing into so much detail, let us now follow the procedure on commencement of each working period; we shall then describe some ancillary equipment.

First of all the two rotary vacuum pumps are started up, and the water supply for the high-vacuum pumps is turned on; voltage is then applied to the heaters of the pumps. The pumps acquire their normal working temperature in about $3/4$ hour, $1/4$ of an hour later the pump valve may be opened.

In the meantime the refrigerator for the vapour traps will have been started up, and the filament heater supply for the oscillator valves producing the Dee voltage, as well as that for the rectifier valves supplying anode voltage for the oscillator are then switched on; a delay of about 20 minutes is necessary before these valves can be put into operation. Cooling water for the oscillator anodes and the whole of the oscillator circuit including the Dees is next applied. If necessary, the tungsten pin in the ion source is renewed. The target, previously loaded with the required substance, is then introduced and connected to the cooling system. The rotary capacitor in the modulator is allowed to come up to its required speed, as well as the generator supplying the energizing current for the large magnet, and its field dynamo. The operation of opening the valves for the supply of cooling oil and water for the electromagnet unlocks a switch in the generator field circuit, which is next closed, and the current
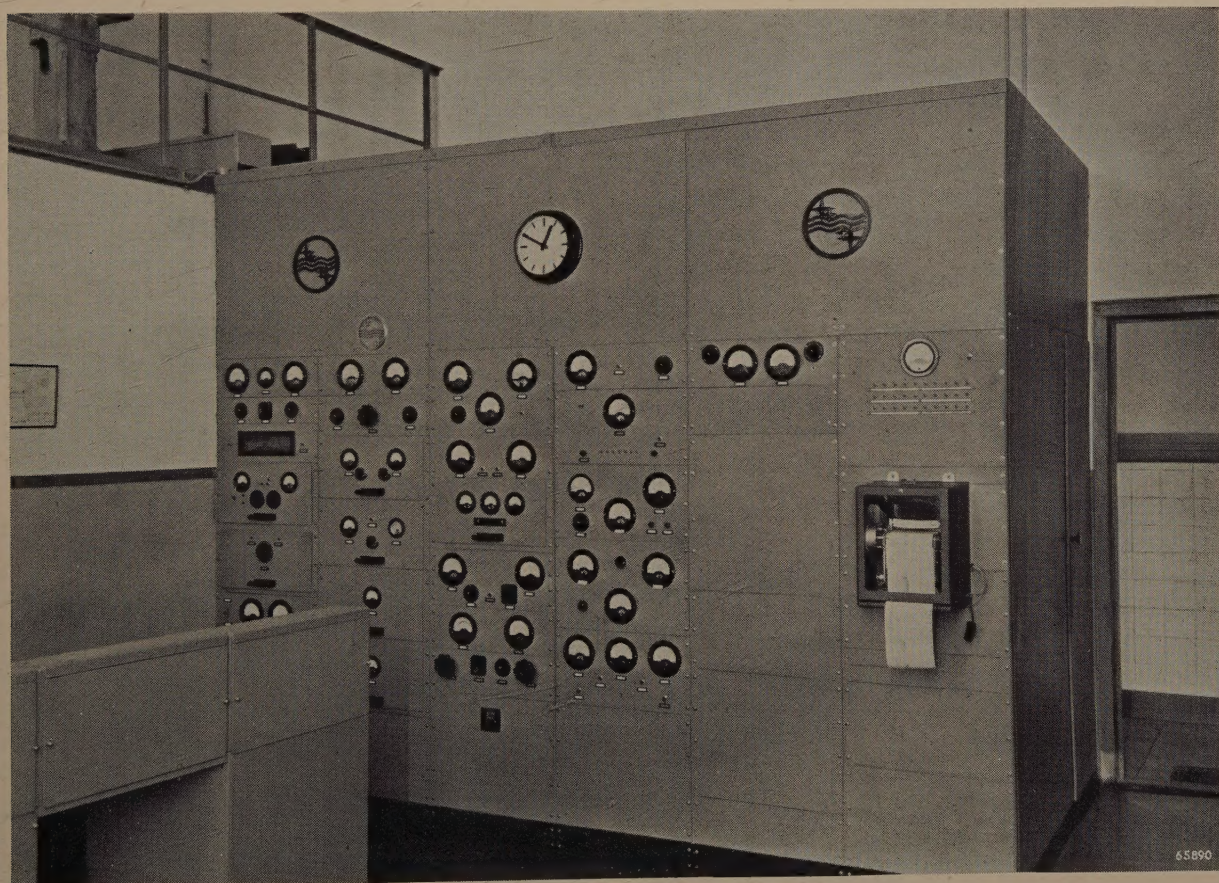

Fig. 20. The main panels in the control room of the synchrocyclotron, with switches, meters etc. for operating and monitoring the more important functions, viz. left to right: energizing of the magnet with stabilization and temperature monitoring device; anode voltage for the H.F. oscillator (with automatic cut-out); H.F. oscillator control (frequency measurement etc.); voltage and gas supply to the ion source and sundry other monitoring and control circuits such as on the speed of the modulator, the pumps, the continuous recording of the beam current and warning signals,.

in the coil is adjusted to the correct value. The 500 V d.c. will in the meantime have been applied to the Dees, thus neutralizing possible discharge in the acceleration chamber (see II). At this stage voltage is applied to the anodes of the oscillator to supply the high frequency field for the Dees. Opening the water supplies to the ion source and target closes another interlock, so that, finally, the voltage can be applied to the ion source; before this is done, however, all personnel must have left the region of the cyclotron, as the beam of accelerated particles is formed and the target commences to produce radiation.

All further adjustments, as well as monitoring all the different elements of the equipment, must then be effected from the control room, which is isolated from the cyclotron by a 3.5 m thick wall of water (*fig. 20*). To commence with, the oscillator is tuned to resonance with the circulating particles, which is done by adjusting the trimming capacitor on the modulator (II, C″, fig. 9) by means of a servo-motor. The oscillator frequency remains reasonably constant and needs readjustment only once or twice during the day, this being done by hand. Other parameters which are subject to greater variation, are stabilized automatically.

Automatic stabilization is especially important for the magnet energizing current (the quotient of the average oscillator frequency and the magnetic flux density in the acceleration chamber must be kept constant within narrow limits [6])). The method of stabilizing this current is illustrated in *fig. 21*. The energizing current passes through a high-stability resistor R (manganin wire resistor in an oil-bath maintained at constant temperature). The voltage across this resistor, in series with a stabilized reference voltage of opposite polarity, is applied to a circuit containing a mirror galvanometer. As long as the energizing current is at its normal value, the beam of light from the galvanometer remains at zero, but, should the current rise or fall by a given amount, the beam falls on one or the other of two photo-electric cells. The photo-current is amplified and applied to a servomotor which corrects the field (and consequently the voltage) of the field dynamo used with the main generator; thus, if the current exceeds the upper limit, the main generator field is accordingly reduced and vice versa. This "discontinuous" method of control has the advantage that it does not operate on variations in the current which are so small that they fall within the limits defined; there is therefore

little risk of "hunting" (continual adjustment backwards and forwards). The greatest variations in the current as stabilized in this manner are within 6×10^{-4}, and it follows from the magnetization curve of the steel (see III, fig. 3) that the flux density is then constant to within about 3×10^{-4}. This degree of stability is even higher than required.

Apart from the interlocking of certain controls already mentioned, the equipment is protected by numerous warning signals. In fig. 20 a series of lamps will be seen on the extreme right-hand panel, just above the instrument for recording the beam current. Should a fault occur in any of the components of the cyclotron, one of these lamps immediately lights as a warning. Faults involving any risk of damage immediately isolate the component concerned. For example, the pumps are automatically shut off in the event of the pressure in the system becoming dangerously high. Similarly, should one of the oscillator valves break down, the anode voltage is at once cut off; this is effected by means of the kind of repeater circuit employed in broadcasting transmitters: anode voltage is applied again automatically a few seconds later, to check whether the interruption is only transient; if flashover again occurs, the cut-out again opens, but after this,
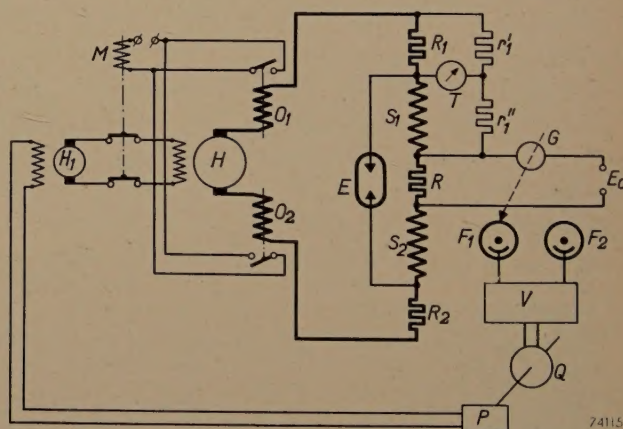

Fig. 21. The energizing circuit of the large electromagnet. S_1 and S_2 are the two large energizing coils, permanently connected to the generator H of the energizing current (500 V, approx. 175 A); H_1 field-exciter dynamo for the generator H; O_1, O_2 cut-outs operating on current overload, which break the circuit of H_1 through an electromagnetic switch M; E rare gas fuse for protection of the coils. The energizing current is stabilized by means of a mirror galvanometer G which measures the difference between the voltage across a resistance R and a constant reference voltage E_0. According to the position of the galvanometer light beam, two photo-electric cells F_1 F_2, by means of an amplifier valve V and a servomotor Q, control the rectifier P which excites the field dynamo H_1. The galvanometer is protected against heavy current surges, particularly when the main circuit is closed and opened, by a rather complicated device not shown in the diagram. By means of a manganin strip R_1 and resistors r', r'', which together with the coil S_1 form a bridge circuit, and of the micro-ammeter T, the temperature of the coil S_1 is monitored continuously (a similar arrangement is provided for coil S_2).

[6]) See W. de Groot, Cyclotron and synchrocyclotron, Philips tech. Rev. **12**, 65-72, 1950.

the voltage will have one more "try"; only if the same result is obtained this time, is the anode voltage cut off finally and the fault has to be traced and rectified.

Mention should also be made of the special precautions taken to safeguard the energizing coils of the magnet. In view of the enormous amount of energy stored in the field of the magnet (theoretically 650 000 Wsec (see III) but in reality, in view of stray fields, even higher), care must be taken to ensure at all costs that the energizing circuit is never broken; the resultant high potential across the coils would otherwise have catastrophic consequences. In the first place, therefore, the coils are permanently connected to the generator (fig. 21). The only switch used is in the field circuit of the generator, as will already have become clear to the reader. Further there are no fuses between the coils and the generator. To protect the generator itself against possible short-circuiting of the energizing circuit, this circuit includes an overload-current relay for isolating the field dynamo from the main generator. The magnet coil circuit is thus not interrupted and the magnetic energy can leak away gradually through the generator. Connected in parallel with the coils, moreover, is a rare-gas fuse whose electrodes are held under presssure by a heavy spring; should the connection between the generator and the coil at any time be open-circuited, the rising voltage will ignite the gas-filled fuse. This in itself will provide a path for the discharge of the energy, but the resistance of this path is reduced in a matter of seconds because the glass discharge tube softens as a result of the heat developed and is telescoped by the spring. The electrodes then constitute an effective short-circuit for any further rise in the voltage on the coils.

————

Summary. Continuing with the earlier articles on the oscillator, modulator and electromagnet of the Philips synchrocyclotron at Amsterdam, a description is now given of the other important components, viz. the acceleration chamber, the Dees, the ion source, target, vacuum pump and some of the controls and protective devices. The circular, evacuated acceleration chamber, nearly 2 metres in diameter, comprises 7 cm thick top and bottom plates of the steel of which the magnet is made; for the rest it is built up in situ, of conveniently small members, so that it can at all times be dismantled completely or in part. The vacuum joints are sealed with rubber strip and the total air leakage amounts to only 6 litres per week. At the gap between the Dees the height of the Dee is 20 cm, to allow of the collection of as many ions as possible to form the beam and to ensure that few will be lost as a result of collisions arising from the vertical oscillations. The ion source consists of a chamber to which heavy hydrogen is supplied at a pressure of about 0.1 mm Hg; this passes subsequently through a communicating duct 5 mm in width to the acceleration chamber. A gas discharge is maintained in the ion source which results in a highly concentrated jet of electrons being sent into the acceleration chamber. The way in which this empirically devised mechanism functions cannot yet be fully explained, but the very copious supply of ions thus obtained is largely responsible for the high yield of radio-active materials which the equipment produces. The most satisfactory position of the ion source between the Dees can be found while the cyclotron is working. The target, in which a good 500 W of power is dissipated, is thoroughly water-cooled. The temperature of the cooling-water, which may be measured and recorded continuously, is a direct measure of the beam current. Both the ion source and the target are introduced into — and withdrawn from — the acceleration chamber through traps. The acceleration chamber is permanently connected to a 4-stage high-vacuum pump having an unbaffled pumping speed of 3500 litres of air per second or, as measured at the chamber, 2200 l/sec. A control room, which is isolated from the cyclotron by a wall of water 3.5 m thick, houses a number of controls and switches for monitoring and adjusting the working of all components during the operation. The energizing current for the magnet is automatically kept at a constant value by a stabilizing system using a mirror-galvanometer and two photo-electric cells. Possible faults in a number of components of the cyclotron are indicated by means of signal lamps, or, in the event of serious breakdown, the component is automatically isolated. Errors in manipulation are prevented by a number of interlocking systems.

———

ABSTRACTS OF RECENT SCIENTIFIC PUBLICATIONS OF THE N.V. PHILIPS' GLOEILAMPENFABRIEKEN

Reprints of these papers not marked with an asterisk * can be obtained free of charge upon application to the address on the back cover.

2008: J. C. F r a n c k e n: Opneembuizen voor televisie, III. Electronenoptische problemen in de beeldiconoscoop (T. Ned. Radiogenootschap **16**, 243-257, 1951, No. 5). (Television camera tubes, III. Electron-optical problems in the image iconoscope; in Dutch).

In the image-iconoscope two parts can be distinguished: the scanning section and the electron-image section. In the design of both parts typical electron-optical problems are involved. With respect to the scanning section, means to obtain nearly uniform focus over the target are discussed. It appears to be advantageous to use a high-current density at the cathode. Therefore, use is made of the so-called L-cathode which also allows for accurate mounting of the gun parts. The electron-image section consists of the photocathode, an electron lens and the target. The elec-

tron lens is formed by co-axial electrostatic and magnetic fields. The electrostatic field exists between cathode and anode cylinder, the magnetic field is generated by a rather long coil. The properties of this system are discussed. Causes of unsharpness (chromatic aberration and curvature of the field) and geometric distortion (pin-cushion and S-distortion) are mentioned. All these errors can be reduced to such an extent that a satisfactory image can be obtained. A special feature of this type of electron lens is the possibility of varying the magnification of the image continuously without affect its sharpness and rotation. This can be done by using a coil split up into three separate sections. By varying the currents in these sections simultaneously, a continuous variation of the magnification in a range of 1 : 2 can be achieved (see Nos. **2006** and **2007**).

2009 *: P. Schagen: On the image iconoscope, a television camera tube (Thesis, Amsterdam 1951, 89 pp, 40 figs.).

After a short historical introduction and a brief discussion (Ch. I) of modern television camera tubes, a simplified theoretical approach is given in Ch. II to the processes involved in building up the potential image on the target of the image iconoscope by the photo-electrons, and the way in which the video-signal is created when the potential image is removed by the scanning beam. This theory, based on some hypotheses concerning the behaviour of secondary electrons, leads to expressions for the potential of a target element as a function of the photo-electric current.

In Ch. III the methods are described with which the signal output and the secondary-emission coefficient of the target have been measured.

The theoretical results are compared with the measurements in Ch. IV and some conclusions are drawn with respect to the steps which can be taken to improve the characteristics of the tube. It appears that the resulting experiments confirm the theoretical predictions.

In Ch. V a method is described which considerably reduces spurious signals in the video-signal produced by the image iconoscope, and enables a line-by-line restoration of the black-level.

Finally, in Ch. VI, the performance of the image iconoscope is discussed in comparison with other camera tubes as regards the relation between image signal and photo current, effective time of illumination, spurious signals, simplicity of operation and focussing, spectral sensitivity, stability, black-level, variable magnification, depth of focus, signal-to-noise ratio and sensitivity. Attention is drawn to the fact that sensitivities are to be compared by comparing the illumination levels needed for producing images of good quality with corresponding depth of focus and noise.

The conclusion is drawn that the Philips image iconoscope is a very good tube for studio work as well as for outdoor work in daylight. For illuminations below 1000 lux the quality of the image may be insufficient for broadcasting purposes. This might be improved by producing a tube with a larger photocathode.

2010: J. M. Stevels: La coloration du verre (Verres et Réfractaires, **5**, 197-204, 1951, Aug.). (The colouring of glass; in French.)

The colouring of glasses is determined:
1) by the slope of the absorption curve, 2) the presence of atoms having a specific absorption, 3) by electronic transitions between cations. The location of the slope of the absorption curve is determined by the Madelung potential at the place of an oxygen ion. This potential itself depends on the location of the oxygen ion and on the charge of the network forming ions. Admitting as such the ions P^{5+}, Si^{4+} and B^{3+}, one finds six possible positions of the absorption curve.

The absorption caused by ions with specific absorption in the visible spectrum essentially depends on their location in the lattice (network former or network modifier).

Transitions between cations (network former or modifier) complicate the absorption problem. This phenomenon presents itself especially if one sort of ion occurs with two different valencies. The case Fe^{3+}, Fe^{2+} is representative and very instructive in this respect.

2011: E. J. W. Verwey: Ver-reikende krachten in colloïd-chemische en biochemische systemen (Hand. Nat. Geneesk. Congres 32, 4-14, 1951). (Long distance forces in colloidal and bio-chemical systems; in Dutch).

This lecture deals with the forces, attractive (London-Van der Waals) and repulsive (electric double layer) between colloidal particles (see these abstracts, No. **1769**) and with the question of stability of colloids. The same considerations are tentatively applied to bio-colloids. In this case, beyond general repulsive and attractive forces, there are specific forces, dependent on the structure of the particles. The experiments of Rothen on interaction between antigen and antibody are mentioned as an example. Finally a number of phenomena occurring in hydrophilic colloids are discussed.